UNIVERSIDADE ESTADUAL DE CAMPINAS
FACULDADE DE ENGENHARIA MECÂNICA
E INSTITUTO DE GEOCIÊNCIAS

LORENA CARDOSO BATISTA

INFLUENCE OF INTEGRATION BETWEEN RESERVOIR AND PRODUCTION SYSTEM CONSIDERING POLYMER INJECTION IN A HEAVY OIL RESERVOIR

INFLUÊNCIA DA INTEGRAÇÃO ENTRE RESERVATÓRIO E SISTEMA DE PRODUÇÃO CONSIDERANDO INJEÇÃO DE POLÍMERO EM UM RESERVATÓRIO DE ÓLEO PESADO

CAMPINAS
2024

LORENA CARDOSO BATISTA

INFLUENCE OF INTEGRATION BETWEEN RESERVOIR AND PRODUCTION SYSTEM CONSIDERING POLYMER INJECTION IN A HEAVY OIL RESERVOIR

INFLUÊNCIA DA INTEGRAÇÃO ENTRE RESERVATÓRIO E SISTEMA DE PRODUÇÃO CONSIDERANDO INJEÇÃO DE POLÍMERO EM UM RESERVATÓRIO DE ÓLEO PESADO

Master's thesis presented to the School of Mechanical Engineering and Institute of Geosciences of the State University of Campinas in partial fulfillment of the requirements for obtaining the degree of Master of Science in Petroleum Science and Engineering, in the area of Reservoirs and Management.

Dissertação de Mestrado apresentada à Faculdade de Engenharia Mecânica e Instituto de Geociências da Universidade Estadual de Campinas como parte dos requisitos exigidos para obtenção do título de Mestra em Ciências e Engenharia de Petróleo, na área de Reservatórios e Gestão.

Orientador: Prof. Dr. Denis José Schiozer
Coorientador: Dr. João Carlos von Hohendorff Filho

Este exemplar corresponde à versão final da Dissertação defendida pela aluna Lorena Cardoso Batista e orientada pelo Prof. Dr. Denis José Schiozer.

CAMPINAS

2024

Ficha catalográfica
Universidade Estadual de Campinas (UNICAMP)
Biblioteca da Área de Engenharia e Arquitetura
Rose Meire da Silva - CRB 8/5974

B32i

Batista, Lorena Cardoso, 1999-
Influence of integration between reservoir and production system considering polymer injection in a heavy oil reservoir / Lorena Cardoso Batista. – Campinas, SP : [s.n.], 2024.

Orientador: Denis José Schiozer.
Coorientador: João Carlos von Hohendorff Filho.
Dissertação (mestrado) – Universidade Estadual de Campinas (UNICAMP), Faculdade de Engenharia Mecânica.

1. Injeção de polímero. 2. Óleo cru. 3. Simulação. 4. Integração de sistemas. I. Schiozer, Denis José, 1963-. II. Hohendorff Filho, João Carlos von, 1976-. III. Universidade Estadual de Campinas (UNICAMP). Faculdade de Engenharia Mecânica. IV. Título.

Informações Complementares

Título em outro idioma: Influência da integração entre reservatório e sistema de produção considerando injeção de polímero em um reservatório de óleo pesado
Palavras-chave em inglês:
Polymer injection
heavy oil
Flow simulation
Production system
Área de concentração: Reservatórios e Gestão
Titulação: Mestra em Ciências e Engenharia de Petróleo
Banca examinadora:
Denis José Schiozer [Orientador]
William Godoy de Azevedo Lopes da Silva
Valdir Estevam
Data de defesa: 13-06-2024
Programa de Pós-Graduação: Ciências e Engenharia de Petróleo

Identificação e informações acadêmicas do(a) aluno(a)
- ORCID do autor: https://orcid.org/0000-0001-9538-3291
- Currículo Lattes do autor: http://lattes.cnpq.br/3660659054938417

UNIVERSIDADE ESTADUAL DE CAMPINAS
FACULDADE DE ENGENHARIA MECÂNICA
E INSTITUTO DE GEOCIÊNCIAS

DISSERTAÇÃO DE MESTRADO ACADÊMICO

INFLUENCE OF INTEGRATION BETWEEN RESERVOIR AND PRODUCTION SYSTEM CONSIDERING POLYMER INJECTION IN A HEAVY OIL RESERVOIR

INFLUÊNCIA DA INTEGRAÇÃO ENTRE RESERVATÓRIO E SISTEMA DE PRODUÇÃO CONSIDERANDO INJEÇÃO DE POLÍMERO EM UM RESERVATÓRIO DE ÓLEO PESADO

Autor: Lorena Cardoso Batista
Orientador: Prof. Dr. Denis José Schiozer
Coorientador: Dr. João Carlos Von Hohendorff Filho

A Banca Examinadora composta pelos membros abaixo aprovou esta Dissertação:

Prof. Dr. Denis José Schiozer, Presidente
FEM / UNICAMP

Prof. Dr. Valdir Estevam
FEM / UNICAMP

Dr. William Godoy de Azevedo Lopes da Silva
Principal Researcher Technology Management – Equinor

A Ata de Defesa com as respectivas assinaturas dos membros encontra-se no SIGA/Sistema de Fluxo de Dissertação/Tese e na Secretaria do Programa da Unidade.

Campinas, 13 de junho de 2024.

DEDICATION

To my mother, Eloane, who has always encouraged and supported me in all my choices.

ACKNOWLEDGEMENTS

To my parents, Eloane and Udivan, for their dedication in getting me this far. I would also like to thank my family, especially Udileusa, Lucidario, and Tafo to his support during my academic journey.

To my husband, Pedro, for all his understanding, affection, and support at every moment I needed it.

I would also like to thank my advisor, Prof. Dr. Denis José Schiozer, for the opportunity to do my master's degree under his guidance and for his support over the years. His guidance and immense knowledge were essential to the preparation and completion of this dissertation.

My sincere thanks to my co-supervisor, Dr. João Hohendorff Filho, who has always been there to pass on his knowledge and enthusiasm about integration, ever since the "Numerical Simulation of Reservoirs" course.

To Dr. Vinicius Botechia, for all his help in carrying out this work. I would also like to thank Prof. Dr. Valdir Estevam for sharing all his knowledge about nodal analysis and ESPs.

To my friends at CEPETRO, especially Marx, Rafaela and João, for their partnership and for making this period lighter. I also thank my friends from Pará.

To the researchers and staff at UNISIM, CEPETRO, and at the Division of Petroleum Engineering for their technical support.

To the financial support of FAPESP (grant #2022/02231-9), São Paulo Research Foundation.

Finally, I would like to thank EPIC, Equinor Brazil, and Energi Simulation for their financial and technical support. I would also like to thank Schlumberger (SLB) for the software licenses.

“The mind that opens to a new idea never
returns to its original size.”

Albert Einstein

RESUMO

Estudos de simulação numérica de injeção de polímeros são amplamente relatados na literatura, contudo, a avaliação da injeção de polímeros considerando a integração com o sistema de produção (PS), muitas vezes, é negligenciada ou simplificada, o que pode levar a previsões imprecisas de produção de petróleo. O objetivo deste trabalho foi avaliar o impacto da integração entre o reservatório e sistema de produção, considerando cenários de injeção de polímeros em um reservatório de óleo pesado. Foi utilizado um modelo de reservatório, denominado EPIC001, com características de um campo de óleo pesado marítimo, brasileiro, caracterizado por alta permeabilidade e porosidade. Um modelo de fluido *Black-oil* foi utilizado, considerando óleo pesado (13° API). A estratégia inicial para o campo consistiu em quatro poços produtores e três poços injetores. O sistema de produção abrangeu os poços, linhas de escoamento, e linhas de superfície, até o separador de fluidos. Para integrar o reservatório com o SP, foi utilizada a abordagem de integração desacoplada através de tabelas de desempenho de fluxo vertical. Modelos integrados (IM) foram baseados em modelos de SP simples selecionados inicialmente para o caso. Os resultados foram comparados com modelos sem integração (modelos não integrados - NIM), com condições de contorno baseadas no valor alvo da pressão no fundo do poço (BHP) designado para este projeto. Este estudo foi composto por seis etapas: (1) um SP foi modelado com base em dados encontrados na literatura e definidos para este projeto para ser usado no modelo integrado (IM1); (2) o modelo IM1 foi comparado com o NIM. (3) foi feito um ajuste do sistema de produção do IM1, obtendo o IM2; (4) foi feita uma avaliação do impacto da injeção de polímeros nos modelos IM1 e IM2; (5) foram obtidas as concentrações ótimas de polímero; (6) um modelo baseado em um valor de BHP Revisado foi obtido (NIMr) para alcançar resultados semelhantes aos do IM1. As simulações usando IM1 resultaram em menor produção em comparação com NIM. A redução foi de 22% para injeção de água e 41% para injeção de polímeros, com uma concentração de 2,49 kg/m³. A análise de sensibilidade da concentração de polímero revelou que 1,0 kg/m³ era a concentração mais favorável para o NIM, mas para o IM, a concentração ótima de polímero variou de 0,5 até 1,2 kg/m³, dependendo da configuração dos estágios da bomba e aspectos econômicos. Estas diferenças estão diretamente associadas à influência do sistema de produção nas condições de contorno do reservatório. Quando essas condições são modificadas, elas afetam a produção e escoamento no reservatório. Também foi observado que uma análise mais detalhada das bombas nos permitiu atingir e até mesmo superar a meta de produção estabelecida para o NIM. A abordagem de BHPs revisados levou a uma produção compatível com o caso

integrado, com diferenças alcançando 2,5%. Portanto, os resultados apresentados neste trabalho mostram a importância de considerar a integração para uma previsão precisa da produção de petróleo em simulações de reservatórios, especialmente em cenários envolvendo injeção de polímeros em reservatórios de óleo pesado. Também foi apresentado um exemplo de como isso pode afetar as decisões, mostrando como a concentração ótima de polímero pode mudar dependendo do modelo e das características do sistema de produção. Portanto, considerar a integração é crucial para melhorar a qualidade de decisões e estratégias operacionais.
Palavras-Chave: injeção de polímero; óleo pesado; simulação numérica; integração; sistema de produção.

ABSTRACT

Numerical simulation studies of polymer injection are widely reported in the literature, but the evaluation of polymer injection considering integration with the production system (PS) is often neglected or simplified, which can lead to inaccurate oil production forecasts. The aim of this work was to evaluate the impact of integration between the reservoir and the production system, considering polymer injection scenarios in a heavy oil reservoir. A reservoir model was used, called EPIC001, with the characteristics of a Brazilian maritime heavy oil field, characterized by high permeability and porosity. A Black-oil fluid model was used, considering heavy oil (13° API). The initial strategy for the field consisted of four producers and three injector wells. The production system included the wells, flowlines and surface lines, up to the fluid separator. To integrate the reservoir with the PS, a decoupled integration approach was applied using vertical flow performance tables. Integrated models (IM) were based on simple PS models initially selected for the case. The results were compared with non-integrated models (NIM), with boundary conditions based on the target bottomhole pressure (BHP) value assigned to this project. This study consisted of six stages: (1) an SP was modeled based on data found in the literature and defined for this project to be used in the integrated model (IM1); (2) the IM1 model was compared with the NIM. (3) an adjustment was made to the IM1 production system, obtaining IM2; (4) an assessment was made on the impact of polymer injection on the IM1 and IM2 models; (5) the optimum polymer concentrations were obtained; (6) a model based on a Revised BHP value was obtained (NIMr) to achieve results similar to those of IM1. The simulations using IM1 resulted in lower production compared to NIM. The reduction was 22% for water injection and 41% for polymer injection, with a concentration of 2.49 kg/m^3. The sensitivity analysis of the polymer concentration revealed that 1.0 kg/m^3 was the most favorable concentration for the NIM, but for the integrated models, the optimum polymer concentration varied from 0.5 to 1.2 kg/m^3, depending on the configuration of the pump stages and economic aspects. These differences are directly associated with the influence of the production system on the reservoir's boundary conditions. When these conditions are modified, they affect the production and flow in the reservoir. It was also observed that a more detailed analysis of the pumps allowed us to reach and even exceed the production target set for the NIM. The revised BHPs approach led to a production rate compatible with the integrated case, with differences reaching 2.5%. Therefore, the results presented in this work underscore the importance of considering integration for accurate oil production prediction in reservoir simulations, especially in scenarios involving polymer injection in heavy oil reservoirs. An example of how

this can affect decisions was also presented, showing how the optimum polymer concentration can change depending on the model and production system characteristics. Therefore, considering integration is crucial to improve the quality of operational decisions and strategies.
Keywords: polymer flooding, heavy oil, numerical simulation, integration, production system.

LIST OF FIGURES

LIST OF TABLES

NOMENCLATURE

AC	Abandonment Cost
API	American Petroleum Institute
BHP	Bottom-hole Pressure
EOR	Enhanced Oil Recovery
EPIC001	Reservoir Model Name
ESP	Electrical Submersible Pump
FPSO	Floating Production, Storage and Offloading Unit
IM	Integrated Model
IM1	Integrated Model 1
IM2	Integrated Model 2
IPR	Inflow Performance Relationship
NCF	Net cash flow
NIM	Non-Integrated Model
NIMr	Non-Integrated Model - Revised
OC	Operational Costs of Production
OPR	Outflow Performance Relationship
PS	Production System
STM	Mixed Number of Stages (8-15 stages)
ST20	20 Stages
ST37	37 Stages
ST50	50 Stages
ST80	80 Stages
VFP	Vertical Flow Performance
WC	Water cut

LIST OF SYMBOLS

a	Constant related to gas molecule attraction
b	Constant associated with gas molecule volume
B_g	Gas Formation Volume Factor
B_o	Oil Formation Volume Factor
B_w	Water Formation Volume Factor
$\mathrm{C_{iw}}$	Water injection capacity
$\mathrm{C_{nw}}$	Number of wells capacity
$\mathrm{C_{pl}}$	Liquid production capacity
$\mathrm{C_{po}}$	Oil production capacity
$\mathrm{C_{pw}}$	Water production capacity
dP/dL	Pressure loss rate per unit length
f_w	Water Fractional Flow
g	Gravity Acceleration
$\mathrm{Inv_{plat}}$	Investment in the platform
k	Permeability
k_o	Effective Oil Permeability
k_{or}	Oil Relative Permeability
k_w	Effective Water Permeability
k_{wr}	Water Relative Permeability
M	Mobility Ratio
μ	Fluid Viscosity
μ_o	Oil Viscosity
μ_w	Water Viscosity
p	Gas Pressure
Pe	Reservoir Pressure
ϕ	Porosity
Pwf	Bottom-Hole Pressure
q_m	Mass Flow Rate
∇p	Pressure Gradient
R	Ideal Gas Constant
R_s	Solubility Ratio
RC	Reservoir Conditions

ρ_g	Gas Density
ρ_o	Oil Density
ρ_w	Water Density
SOR	Saturation of Oil Residual
S_t	Total Social Taxes
T	Corporate Tax Rate
T	Temperature
$\nabla \cdot (\rho\vec{u})$	Mass Flow Divergence
∂	Partial Derivative with Respect to Time
V	Gas Volume
V_b	Control Volume
V_g	Gas Volume
V_o	Oil Volume
V_w	Water Volume
$\vec{u}$	Darcy Velocity
λ	Mobility

TABLE OF CONTENTS

1 INTRODUCTION

Advanced recovery techniques, most commonly EOR (enhanced oil recovery), aim to increase oil recovery compared to conventional recovery techniques, such as water or immiscible gas injection. In this context, polymer injection is a chemical EOR method that can be used in heavy oil reservoirs. The polymer is added to water and increases its viscosity for a better sweep efficiency (Li et al., 2014; Rellegadla et al., 2017). The injection fluid, with its modified rheology, is injected into the porous medium, usually in banks.

The efficiency of polymer injection is commonly affected by several factors, such as the injection scheme, the injection start time in relation to the well's production history, and the effects linked to the porous medium, such as adsorption or degradation resulting from shear in the pore throats (Abidin et al., 2012). Reservoir heterogeneities can also have a major impact on the polymer injection process, as they can form preferential paths or delay the polymer advance front in the reservoir (Jia, 2018). Commercial numerical simulators can model many of these effects in porous media. In addition to the porous medium, when the reservoir includes several producing wells that are interconnected in a production system (PS), operational control decisions taken at each well can impact the overall efficiency of recovery in the field. This means that well variables, which are generally the boundary conditions of reservoir simulations, can modify how the polymer advance front is distributed and, consequently, the sweep efficiency. Furthermore, each part of the process involves uncertainties that can affect the reliability of the simulations and, thus, the final decision.

In reservoir simulators, wells are typically represented as sources (or sinks) located within specific cells of the simulation grid. This modeling approach is primarily employed due to the relatively small size of the well compared to the reservoir (Ding et al., 2014). Additionally, integrating these two domains (production and reservoir) is complex due to the differing temporal and spatial scales, which can lead to unique fluid dynamics. Constraints within the wells are commonly established as boundary conditions, regulating parameters such as total flow rate or well pressure.

However, the analysis of total production, just through simulation in the porous medium, cannot capture important effects that occur in the fluid lifting process, flowlines, and platform installations. Furthermore, both well and the reservoir conditions can undergo significant alterations due to the injection and production of diverse fluids. This may lead to modifications in the inflow performance relationship (IPR) and outflow performance relationship (OPR) curves, thereby altering the well pressure condition in wells.

Therefore, it is important to consider the flow conditions not only within the reservoir but also throughout the entire production system. The decoupled integrated approach modeling is essential for optimizing production efficiency and maximizing oil recovery.

1.1 Motivation

Numerous studies reporting integrated simulation between the reservoir and the production system highlight the importance of integration to properly forecast the oil production (Ghorayeb et al., 2003; Hiebert et al., 2011; Hohendorff Filho and Schiozer, 2022a; Kharisov et al., 2012; Rotondi et al., 2008; Su et al., 2016; Victorino et al., 2018, 2022).

To the best of our knowledge, however, few works evaluate the integration impact considering the scenarios of polymer injection in heavy oil reservoirs. Polymer injection poses several challenges, such as the limits achieved in injectors and the changes in water cut after water flooding. The lack of a properly integrated simulation may also lead to incorrect operational decisions and predictions, resulting in production losses, increased costs, or inaccurate production forecasts. Therefore, it is crucial to study the integration of the production system in heavy oil reservoirs subjected to polymer injection as an EOR technique.

1.2 Objectives

The objective of this work is to investigate the influence of integration between reservoir and production system on final oil recovery in the context of a heavy oil field undergoing polymer flooding, modeled in the ECLIPSE™ simulator. The integration approach employed is based on the decoupled methodology, which uses vertical flow performance (VFP) tables generated within a production system simulator, PIPESIM™.

1.3 Organization

This work was structured into seven chapters. Chapter 1 begins with a general introduction to the project and the importance of integration between reservoirs and production systems, as well as the motivation and objectives of the study. Chapter 2 provides the theoretical background. In Chapter 3, a comprehensive literature review of published works addressing the integration between reservoirs and production system and the polymer injection technique is presented. Chapter 4 presents the general methodology adopted to analyze the influence of polymer injection on the decoupled integration between reservoir and production system. Chapter 5 shows the application. In Chapter 6, the main results and discussion obtained is presented. Finally, in Chapter 7, the conclusions obtained from the development of this study are presented, as well as recommendations and ideas for future research.

2 THEORETICAL BACKGROUND

In this chapter, it is presented the most relevant theoretical concepts for understanding advanced recovery methods, polymer injection and the integration between reservoir and production systems.

2.1 Recovery Methods

In the initial stage of production in an oil field, fluids are extracted from the reservoir rock through wells, driven by the natural energy of the petroleum system. However, the production rate typically declines rapidly, resulting in recovery of only a small fraction of the original oil in place. To prevent a rapid drop in reservoir pressure (which causes a reduction in oil production), oil recovery methods have emerged with the aim of extending the productive life of a field and improving oil recovery. These techniques are applied in fields that are in a phase of production declining. However, depending on some conditions and factors, such as production time and barrel price, recovery techniques can be used even in the initial production phase. The recovery methods are generally divided into three main classifications: primary recovery, conventional methods, and special recovery methods or EOR (Isaev et al., 2022).

Primary recovery involves the initial extraction of hydrocarbons from a reservoir through natural reservoir pressure, without the aid of external fluids injected into the reservoir. Conventional recovery methods, such as immiscible gas injection and water injection, are employed to increase the energy within the reservoir. The injected fluid mechanically displaces the oil in the porous media by inducing a pressure gradient from the injectors towards the producers. However, in some reservoirs, such as heavy oil fields, water injection may not be effective due to unfavorable fluid mobility relationships. In these cases, EOR techniques can be considered, to increase the sweeping efficiency. There are three main types of EOR methods. Thermal methods involve increasing the temperature of the reservoir to reduce the oil viscosity. Miscible EOR methods involve the injection of solvents (typically gases above the minimum miscibility pressure) that interact with hydrocarbons, changing their thermodynamic properties and reducing interfacial tensions between the solvent and the oil, thus decreasing residual oil saturation. Chemical EOR methods involve adding chemicals to the injected water to improve the mobility ratio (such as polymer injection) or decrease interfacial tension (such as surfactants or alkaline solutions) (Rosa et al., 2006).

Among the various Enhanced Oil Recovery (EOR) methods, polymer injection stands out as one of the most extensively employed techniques in the industry. Therefore, in this dissertation, the primary emphasis will be on exploring polymer injection. Next, further details about this technique were discussed.

2.2 Polymer Injection

Polymers are macromolecules formed by chemically bonding numerous smaller units, called monomers, together resulting in complex chains with high molecular weights. Polymer injection is an EOR technique, where polymer solutions are injected into the porous medium, generally alternating the injection between polymer banks and water injection. The injection of a more viscous fluid reduces the mobility of the displacing fluid. As a consequence, there is a more uniform distribution of fluid within the reservoir, enhancing swept efficiency and consequently leading to increased oil recovery (Gbadamosi et al., 2022).

The mobility ratio is defined as presented in Equation 2.1, where the displacing fluid is designated by the subindex “w” referring to water that is generally used in secondary recovery and the subindex “o” refers to the displaced fluid, generally the oil that is contained in the porous medium. Especially in heavy oil reservoirs, this mobility ratio increases, since the viscosity of the oil is much greater than the viscosity of the displacing fluid. When the mobility ratio moves away from 1, it indicates that one of the fluids is easier to flow through the porous medium than the other. While a mobility ratio close to 1 indicates that both fluids will have closer mobilities. The consequence is that the injection front will be more homogeneous in the scenario with a mobility ratio close to 1 and thus the sweep efficiency will be increased and consecutively smaller regions with oil will be remain. The destabilization of the polymer injection front forms the called “viscous fingers” (Thomas, 2019).

$$M = \frac{\lambda_w}{\lambda_o} = \frac{k_w}{k_o}\frac{\mu_o}{\mu_w} = \frac{k_{wr}}{\mu_w}k\frac{k_{\mu_o}}{k_{or}}\frac{1}{k} = \frac{k_{wr}}{\mu_w}\frac{k_{\mu_o}}{k_{or}} \qquad \textbf{Equation 2.1}$$

where M is the mobility ratio; λ_w and λ_o are the water and oil mobility, respectively; k_w and k_o are the effective water and oil permeability, respectively; k_{wr} and k_{or} are the relative water and oil permeability; k is the permeability; μ_w and μ_o are the water and oil viscosity, respectively. The effective permeabilities for oil and water are given by $k_o = k \cdot k_{ro}$ and $\mathrm{k_w} = \mathrm{k} \cdot \mathrm{k_{rw}}$, respectively.

Figure 2.1 illustrates how polymer injection influences oil recovery by reducing the mobility ratio. If M > >1, as illustrated in Figure 2.1 (a), this indicates that water is more mobile than oil. This represents an unfavorable condition, as water forms fingers (phenomenon of viscous instabilities or viscous fingering) across the oil zone, leading to premature breakthrough and lower oil displacement efficiency. Figure 2.1 (b) illustrates the case, where the formation of a more stable displacement front occurs, with a reduced fingering effect (Gbadamosi et al., 2019).

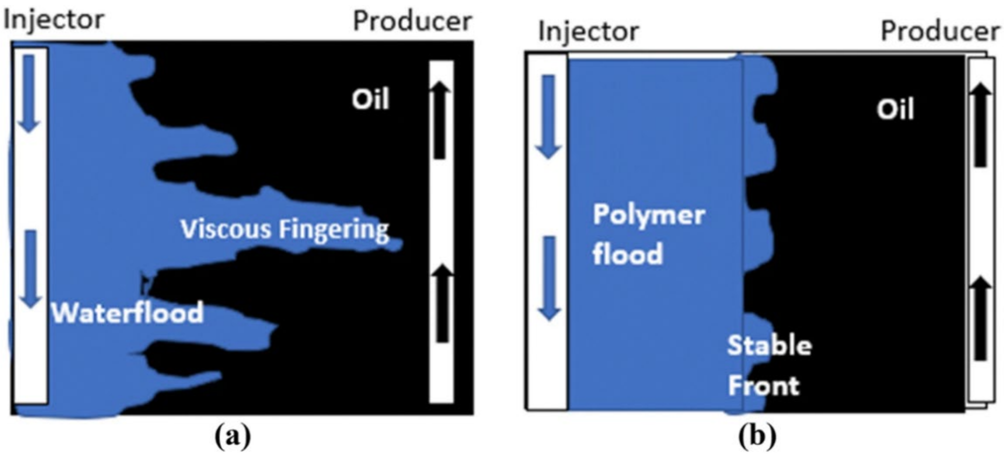

Figure 2.1 – Typical sweep profiles for a process with mobility ratio, (a) M>1 and (b) M<=1 (Gbadamosi et al., 2019).

The effect, resulting from the change in mobility, can also be explained through the concept of fractional flow (f_w), presented in Equation 2.2, obtained from the Buckley-Leverett equation.

$$f_w = \frac{1}{1 + \frac{k_{ro}}{\mu_o}\frac{\mu_w}{k_{rw}}}$$ **Equation 2.2**

When the mobility ratio, presented in Equation 2.1, is substituted in 2.2, Equation 2.3 is obtained.

$$f_w = \frac{M}{M + 1}$$ **Equation 2.3**

where f_w is the fractional water flow.

Figure 2.2 shows the behavior of the fractional flow as a function of the mobility ratio. It is possible to observe that when increasing the viscosity of the displaced fluid, the mobility ratio tends to be reduced, which will promote a drastic reduction in the fractional flow of water, consecutively improving oil production.

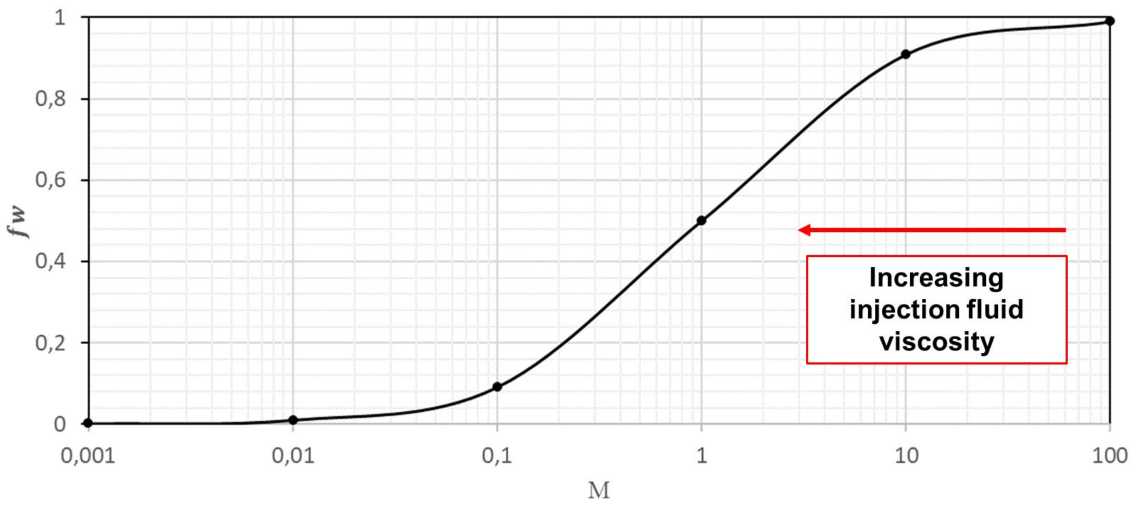

Figure 2.2 – Result of the fractional flow as a function of the mobility ratio M.

2.2.1 Effects Arising from Rock-fluid Interaction

When injecting polymers into the reservoir, several effects resulting from the interaction between rock and polymers, which can affect both the efficiency of the method and the final oil recovery. The main effects include the adsorption of polymers on the rock, the degradation of polymer chains and the decrease in residual saturation (Qin et al., 2020).

Rock-polymer adsorption occurs when polymer molecules interact with the surface of rocks, forming an adsorbed polymer layer. The adsorption of polymers can significantly affect the efficiency of the recovery process and the properties of the injection fluid, since the effective concentration in the bulk of the polymer solution decreases and consequently there is a reduction in viscosity impacting the effective mobility ratio. There are several factors that influence rock-polymer adsorption, including: (a) rock characteristics, such as: mineralogical composition, surface charge and surface area; (b) properties of polymers such as: chemical structure, molecular mass and concentration; and (c) reservoir conditions such as temperature, pressure and salinity of reservoir water. In general, higher temperatures and greater concentrations of salts can promote an increase in the amount of adsorbed polymer. Rock-polymer adsorption can have significant implications for the efficiency of the polymer injection process and oil recovery.

Another important aspect related to the polymer injection process is porous plugging, which can lead to a reduction in rock permeability and consequently diminish injectivity. This phenomenon is quantified mathematically by the skin factor, reflecting additional energy losses near wellbore reservoir region. Increased skin in injectors can reducing injectivity, thereby reducing the volume of fluids that can be injected for recovery (Lopes, 2012).

During flow through the porous medium, polymeric molecules may undergo degradation, impacting the efficiency of the injected fluids viscosity. Mechanisms contributing to degradation include mechanical effects, temperature fluctuations, chemical reactions, and microbial activity. Furthermore, this degradation can compromise the effectiveness of the polymer injection process, resulting in lower oil recovery and a higher proportion of residual oil remaining in the reservoir. Additionally, the degradation of polymeric molecules can escalate operational costs, as larger quantities of polymers, or polymers with greater resistance to degradation, may need to be injected, thereby increasing expenses in the recovery process.

Polymers can also exhibit surfactant properties that, upon interaction with the rock, alter its wettability and can facilitate the reduction of residual oil saturation (SOR). This, coupled with the increased viscosity of the injection fluid and reduced interfacial tension, can lead to enhanced oil recovery and decreased SOR (Qin et al., 2020).

2.3 Modeling and Simulation of Flow in Porous Medium

Reservoir simulation involves the construction of a physical and mathematical model that represents the physical characteristics of the reservoir and simulates the fluid flow and transport processes in the porous medium. By simulating various production scenarios, it is possible to make decisions to optimize oil and gas recovery.

Reservoir simulation aims to represent the complex behavior of fluid flow in porous media as accurately as possible. The reservoir model is generally made up of a set of cells. And properties such as rock permeability, porosity and fluid saturations are assigned to each cell. The governing equations, such as Darcy's law for flow in porous media and the mass conservation of equation, are then solved numerically to simulate fluid flow and displacement processes over time. The simulation offers insights into crucial reservoir parameters, such as pressure distribution, fluid saturations, production rates, and ultimate recovery. The selection of the model to employ relies on the specific characteristics of the simulated processes and the goals of the analysis.

2.3.1 Fluid Modeling

Two main approaches commonly used are compositional modeling and the Black-oil modeling.

Compositional modeling accounts for the detailed composition of fluids within the reservoir, considering various components like light, intermediate, and heavy hydrocarbon fractions. This model is particularly effective for recovery methods that are sensitive to compositional changes in reservoir fluids when the PVT behavior needs to be governed by cubic state functions. Examples of State equations are presented in Equation 2.4 (Redlich-Kwong), Equation 2.5 (Soave-Redlich-Kwong), and Equation 2.6 (Peng-Robinson).

Redlich-Kwong

$$p = \frac{RT}{V-b} - \frac{a/T^{1/2}}{V(V+b)}$$

Equation 2.4

Soave-Redlich-Kwong

$$p = \frac{RT}{V-b} - \frac{a(\mathrm{T})}{V(V+b)}$$

Equation 2.5

Peng-Robinson

$$p = \frac{RT}{V-b} - \frac{a(\mathrm{T})}{V(V+b)+b(V-b)}$$

Equation 2.6

In the given equations, p represents the pressure of the gas; R is the ideal gas constant, which connects the energy scale to the temperature scale in the equation of state for an ideal gas; T signifies the absolute temperature of the system, measured on an absolute scale such as Kelvin; V denotes the volume of the gas, reflecting the space occupied by it; a is a constant related to the attraction between gas molecules, could be dependent of temperature; b corresponds to a constant associated with the volume occupied by the gas molecules themselves.

The compositional model is widely used in simulating chemical processes such as surfactant injection, thermal methods, and miscible gas injection. While compositional modeling provides more accurate results in complex reservoir scenarios, it is computationally demanding, necessitating a substantial dataset and information about fluid properties.

Black-oil modeling is a simplified approach that divides the fluid into three main phases: oil, gas and water. This approach assumes that the phases are immiscible and considers average properties for each phase, such as viscosity and density. More generally, it is assumed that any possible compositional changes are negligible. In this approach, the fluids are at constant temperature and in thermodynamic equilibrium within the reservoir. Under these conditions, the PVT behavior of the system can be expressed by the formation volume factors of oil, water, and gas, respectively B_o, B_w, and B_g, and the mass transfer between oil and gas is described by the solubility ratio R_s. Defined by the equations below:

$$B_o = \frac{[V_o]_{RC}}{[V_o]_{STC}}$$ **Equation 2.7**

$$B_w = \frac{[V_w]_{RC}}{[V_w]_{STC}}$$ **Equation 2.8**

$$B_g = \frac{|\, V_g]_{RC}}{[V_g]_{STC}}$$ **Equation 2.9**

$$R_s = \frac{\lfloor V_{g\ \text{dissolv.}} \rfloor_{STC}}{[V_o]_{STC}}$$ **Equation 2.10**

The specific mass of the oil, water, and gas phases are given by the equations 2.11, 2.12, and 2.13 respectively. The subscript STC, denotes the “standard conditions” and RC reservoir conditions.

$$\rho_o = \frac{1}{B_o}\left(\rho_{oSTC} + R_s \rho_{gSTC}\right)$$ **Equation 2.11**

$$\rho_w = \frac{1}{B_w}\left(\rho_{wSTC}\right)$$ **Equation 2.12**

$$\rho_g = \frac{1}{B_g}\left(\rho_{gSTC}\right)$$ **Equation 2.13**

In the Black-oil model, PVT tables correlate the changes in pressure, volume, and temperature of reservoir fluids. They are typically obtained through experimental methods or by combining Equations of State with experimental data. The PVT data comprises solubility ratio, formation factor and viscosity for both oil and gas phases.

Generally, the flash depressurization is conducted at specific pressure and temperature stages, transitioning a live oil condition with reservoir characteristics to conditions similar to those found in surface tanks and separators.

Black-oil modeling is widely used in industry due to its computational efficiency and ability to provide satisfactory results in a timely manner. This approach will be used in this dissertation, and some specific aspects of this model will be presented in the next section.

2.3.2 Fluid Flow in Porous Media

Darcy's Law, presented in Equation 2.14, describes the flow of fluids through porous media and is a fundamental equation in reservoir simulation. It relates the fluid flow rate to the pressure gradient and rock properties, such as permeability and viscosity.

$$\vec{u} = -\frac{k}{\mu}(\nabla p + \rho \vec{g}) \qquad \textbf{Equation 2.14}$$

where $\vec{u}$ is the Darcy velocity, k is the permeability, μ is the fluid viscosity, ∇P is the pressure gradient in the flow direction, ρ is the fluid density, g is the gravity acceleration.

The conservation of mass equation, also known as the continuity equation, describes the variation in the amount of mass in a system over time. The conservation of mass equation, also called continuity equation, can be expressed for a porous media, as shown in Equation 2.15. In the following equation, $\nabla \cdot (\rho\vec{u})$ represents the divergence of the mass flux, where ρ is the fluid density and $\vec{u}$ is the velocity field, ϕ is the porosity, q_m refers to the mass flow rate related to source or sink term, and V_b is the volume of control over which these processes are being considered.

$$-\nabla \cdot \rho\vec{u} = \frac{\partial}{\partial t}(\rho\phi) - \frac{q_m}{V_b} \qquad \textbf{Equation 2.15}$$

The general equations presented here are generally specified for the model under study and together with other equations, specific to each process, are solved in numerical reservoir simulators. Next, Black-oil model, which was used in this dissertation is discussed.

2.3.3 Black-oil Modeling

In the Black-oil model, the equations are solved considering the compressibility of the fluid for each phase present in the reservoir, such as oil, gas and water. The corresponding flow equations are presented below.

i) Oil Flow equation:

$$\nabla \cdot [\lambda_o(\nabla p_o - \gamma_o \nabla Z)] = \frac{\partial}{\partial t}\left(\frac{\phi S_o}{B_o}\right) - q_o$$

Equation 2.16

ii) Flow of water:

$$\nabla \cdot [\lambda_w(\nabla p_w - \gamma_w \nabla Z)] = \frac{\partial}{\partial t}\left(\frac{\phi S_w}{B_w}\right) - q_w$$

Equation 2.17

iii) Flow equation for the gas phase:

$$\begin{aligned}\nabla \cdot \left[R_s\lambda_o(\nabla p_o - \gamma_o \nabla Z) + \lambda_g\left(\nabla p_g - \gamma_g \nabla Z\right)\right] \\ = \frac{\partial}{\partial t}\left[\phi\left(\frac{R_s}{B_o}S_o + \frac{S_g}{B_g}\right)\right] - R_s q_o - q_{fg}\end{aligned}$$

Equation 2.18

For this equation, λ_l is the general for the mobility of the fluid "l", expressed by Equation 2.19.

$$\lambda_l = \frac{k_{rl}}{\mu_l B_l}k$$

Equation 2.19

The k_{rl} could be also represented as a function of fluid saturation, as showed in Equation 2.20.

$$k_{rl} = k_{rl}(S_l)$$

Equation 2.20

Equation 2.21 and Equation 2.22 represents the capillarity pressures at the oil-water and oil-gas contact, respectively.

$$P_{cow} = p_o - p_w = f(S_w)$$

Equation 2.21

$$P_{cog} = p_g - p_o = f\left(S_g\right)$$

Equation 2.22

Because of the definition of saturation itself, the following restriction equation is derived, as shown in Equation 2.23.

$$S_o + S_w + S_g = 1$$

Equation 2.23

2.4 Production System

The production system comprises the network of lines and equipment facilitating the flow from the reservoir to the surface at a storage or distribution point. It is essential for the production system to be designed to maximize production efficiency while ensuring operational safety. Figure 2.3 illustrates an overview of a production system, formed by two fixed platforms and a FPSO (Floating Production, Storage, and Offloading Unit).

Installed on board an FPSO are the requisite equipment and systems for processing, treating, and storing the oil and gas produced. The utilization of FPSOs presents notable advantages, including operational flexibility, mobility across diverse production fields, cost savings compared to constructing fixed facilities, and the capacity to process and store substantial volumes of oil and gas.

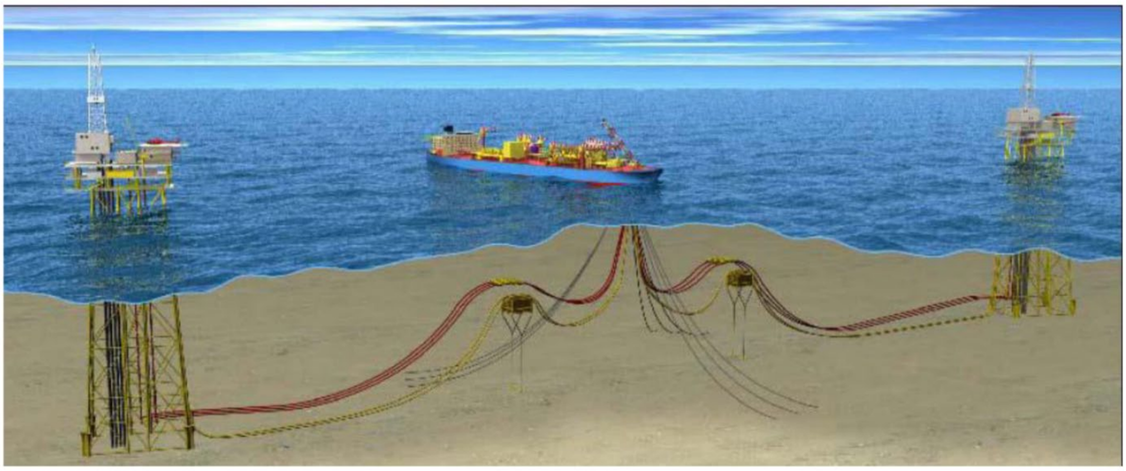

Figure 2.3 – Illustration of a production system consisting of two fixed platforms and an FPSO (Castro et al., 2019).

Additionally, the production system includes subsurface components, as depicted in Figure 2.4, comprising wells, valves, and other subsurface equipment. Wells can be equipped with an artificial lift system, meters, and flow control valves. The configuration of the well can vary depending on its purpose, whether it is for production or injection. Additionally, producers may be converted into injectors due to an increasing water cut or as part of the recovery strategy.

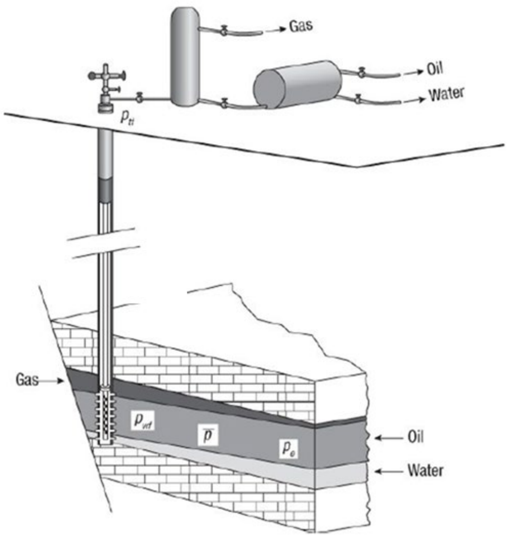

Figure 2.4 – Illustration of the reservoir and production system (subsurface and surface) (Yadigaroglu and Hewitt, 2018).

2.4.1 Energy Loss During the Flow from the Porous Medium to the Platform

The fluid movement, whether in porous media or pipes, is driven by the pressure gradient. The flow always occurs from the region of highest to lower pressure, as a direct consequence of the pressure gradient (as described by Darcy, Bernoulli or in Navier-Stokes equations). Additionally, flow involves energy consumption. As fluid moves through a system (whether porous or free media), it encounters resistance to flow due to factors such as internal friction, turbulence, and changes in the geometry. These resistances result in a pressure reduction along the path taken by the fluid. This loss of energy is known as head loss or pressure loss.

During hydrocarbon production, the fluids flow from the reservoir, normally pressurized as a consequence of natural mechanisms (water influx, gas layer or gravitational segregation) or may be the result of supplementation through conventional or advanced recovery techniques. Therefore, the reservoir is the starting point for oil flow, which then flows through the porous medium towards the producing wells. The flow in the porous medium is governed by reservoir properties such as porosity, permeability, fluid saturation, and compressibility. The loss of energy in porous medium is associated with the dissipation of pressure because of friction along the pores and can be described by the Darcy's Law.

When the fluid arrives at the wells, it is observed a transition from the porous media to the flow in the pipes. Along production lines, energy losses occur due to factors such as friction and turbulence. Furthermore, the presence of valves, bends, connections, and abrupt diameter changes in pipes can lead to additional energy losses.

The pressure at the bottom of the well represents the energy available, coming from the reservoir, to lift the fluids through the production tubing and riser lines up to the surface. In the case where the bottom pressure (p_{wf}) is excessively low, it may be insufficient to transport the fluids to the surface. In this case, artificial lifting strategies can be used. In horizontal or slightly inclined sections, the predominant losses are caused by friction. In the riser sections, losses may be more balanced between the gravitational and frictional components, due to the pressure being already low in these sections. Finally, the flow reaches the production separator, which operates at a working pressure generally between 10 and 20 atmospheres (Andreolli, 2016).

This process, of pressure loss throughout the reservoir and production system, that was described can be illustrated by Figure 2.5. It is possible to observe that the pressure starts at a higher level, reservoir pressure (p_e), and drops as it passes through different points in the system.

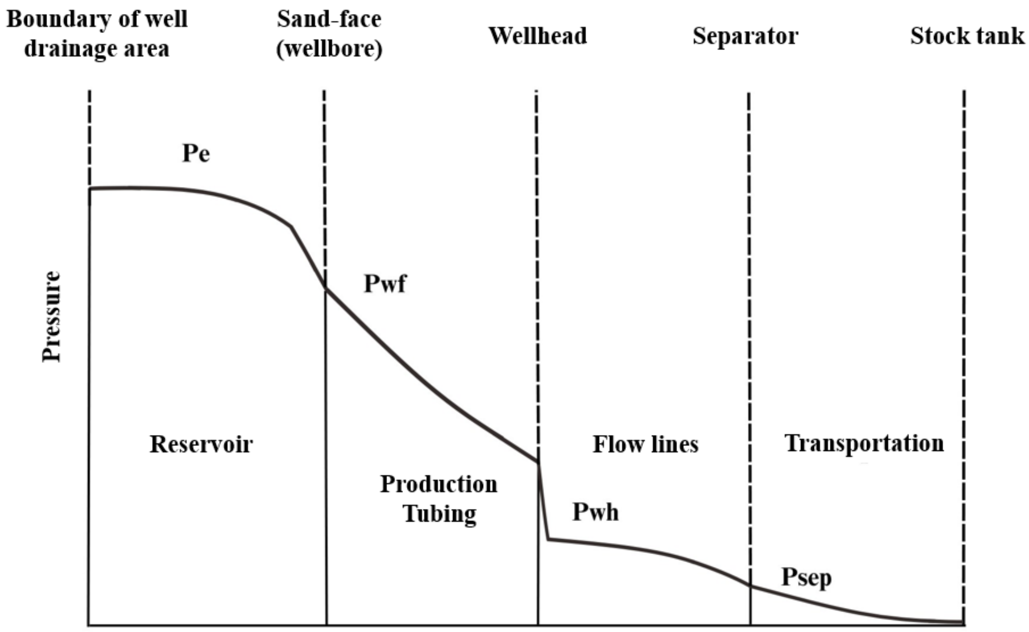

Figure 2.5 – Pressure drops throughout the production system (Jansen, 2017).

2.4.2 Artificial Lift and Submersible Electrical Pump (ESP)

If the fluid reaches the well with less energy than necessary for the lifting process, production will not occur. Thus, artificial lifting methods aim to offer additional energy for lifting fluid or reduce the gravitational and frictional effect during the lifting process.

There are several artificial lift methods used in the oil and gas industry, each with its specific characteristics and applications. Among the main methods, gas lift, mechanical pumping and electrical submersible pump (ESP) stand out.

Pneumatic methods such as Gas Lift are inefficient in the presence of viscous oils (Nguyen, 2020). Of the pumped methods, only the ESP is qualified and was therefore used as the lifting method in this dissertation. However, the following references are recommended for further details on other methods (Andreolli, 2016; Chen, 2017; George Yadigaroglu and Geoffrey F. Hewitt, 2018; Guo et al., 2007; Manshad et al., 2017; Noonan, 2012).

The ESP consists of an electrical submerged centrifugal pump installed inside the production well. The fluid produced is driven by the action of the pump, which generates kinetic energy by accelerating the fluid, providing the pressure necessary to overcome flow resistance and bring it to the surface. Over the last few decades, ESP has proven to be an effective support solution for oil and gas production in different scenarios. Figure 2.6 (a) shows a typical completion, with ESP and Figure 2.6 (b) illustrates the details of two stages ESP pump.

Each stage is made up of a rotor (or impeller) and a diffuser. The rotor is a device fixed to a shaft rotating at high speed (in most common pumps models at approximately 3500 rpm). As the fluid passes through each stage, the rotor accelerates, increasing its kinetic energy, while the diffuser converts this kinetic energy into pressure energy, thereby boosting the pressure of the fluid. The pump efficiency is normally obtained by a performance characteristics curve that are plot showing the relationship between key operational parameters such as head, efficiency, and power consumption across different flow rates for a specific pump model and specific frequency.

Figure 2.7 shows a typical characteristic curve for a submersible pump. The graph plots three different parameters as a function of the flow rate. The head (in units of length), showed by the blue line, represents the height to which the pump can raise the fluid. As the flow rate increases, the head capability of the pump decreases. Efficiency (generally in percentage), depicted by black line, indicates the efficiency of the pump. The curve shows that efficiency increases with flow rate up to a certain point, after which it starts to decline. The peak of the curve represents the Best Efficiency Point (BEP), where the pump operates at its highest efficiency. The power is represented by the red line, illustrates the power requirement for the pump. The power consumption increases with flowrate, which is expected as more energy is required to pump larger volumes of fluid. NPSH stands for Net Positive Suction Head. The term "NPSH required" refers to the minimum pressure required at the suction port of the pump to keep the liquid from cavitating. Cavitation can occur when the pressure in the pump falls below the liquid's vapor pressure, causing bubbles to form and potentially damaging the pump. The shaded yellow area in the background might indicate the preferred operating region for the pump. Operating within this region is often recommended to reduce wear and to operate in more economically oriented scenarios.

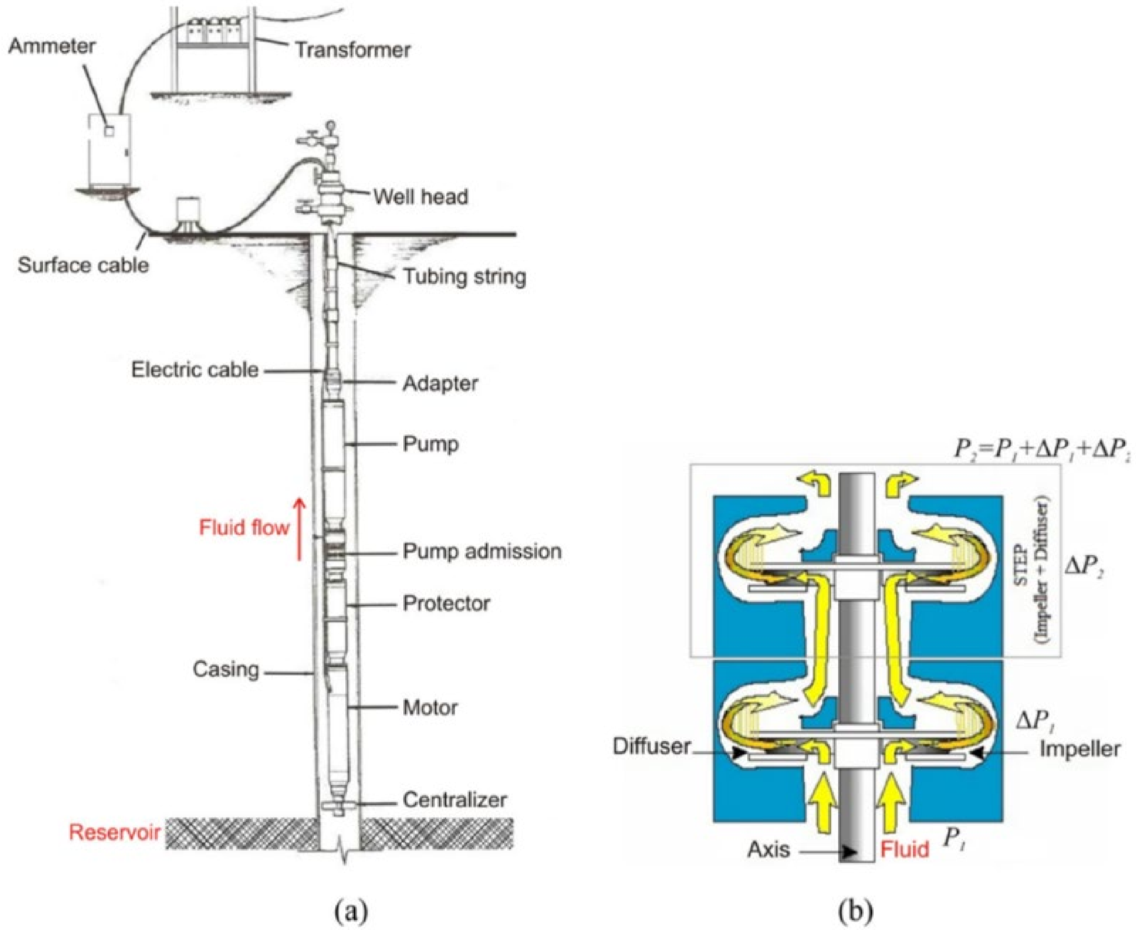

Figure 2.6 – (a) typical centrifugal pump configuration and (b) two stage pump (Joel Romero and Hupp, 2014).

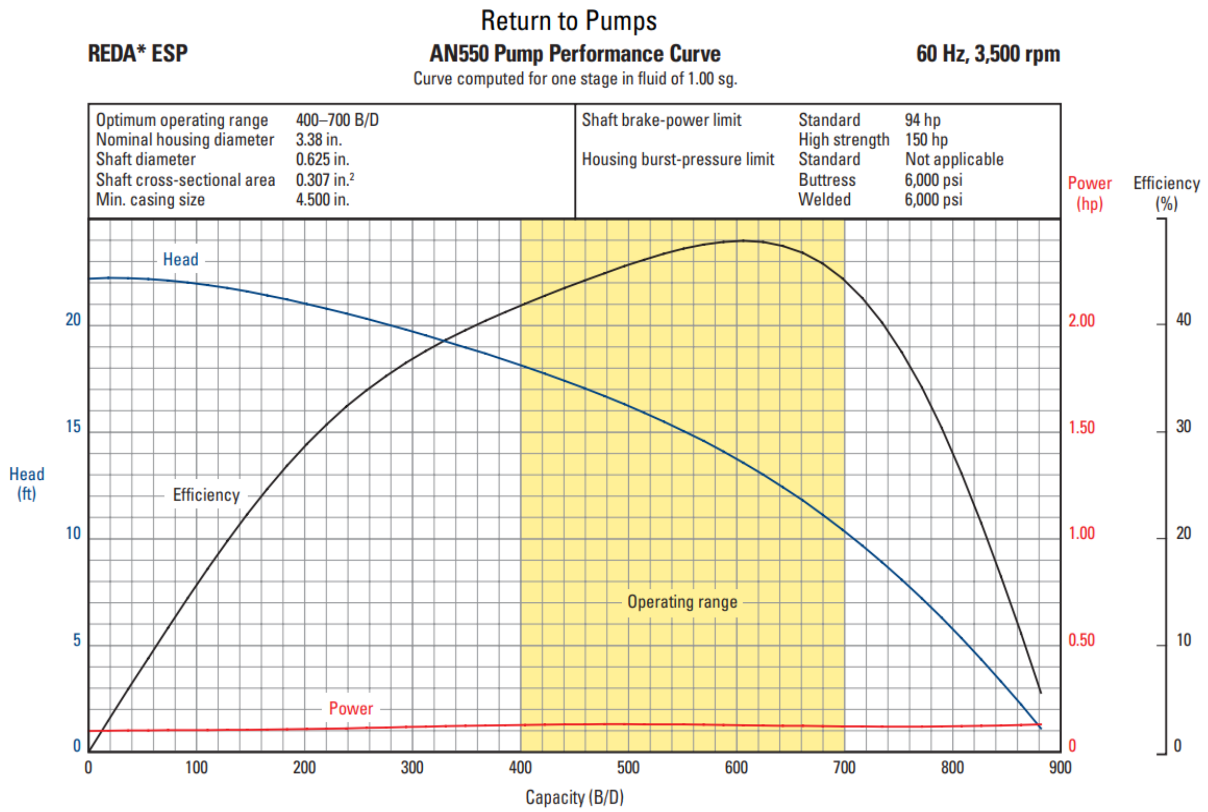

Figure 2.7 – Typical characteristic pump curves (Schlumberger, 2005).

2.4.3 Multiphase Flow in Pipes

As previously discussed, upon reaching the well, the fluid exits the porous medium and initiates its flow through pipes. The governing equations for flow in pipes are conservation of mass, momentum balance and equations of state. Typically, the flow within the well is multiphase, comprising oil, water, and gas phases. In multiphase vertical flow, the phases tend to separate due to differences in density. In the well, the gravitational forces and friction are the largest source of pressure loss. At the time the fluid is elevated, the hydrostatic pressure is reduced, allowing the gas expansion. As a result, the gas and liquid phases do not move at the same velocities, resulting in a high rate of slip between the phases. The gas phase, less dense, more compressible, and less viscous, tends to flow at a higher speed than the liquid phase. For downward vertical flow, such as in injection wells, the liquid often flows faster than the gas due to gravity.

One important aspect is that the distribution of liquid and gaseous phases throughout the flow can assume different patterns commonly observed, as illustrated in Figure 2.8. Predicting the flow pattern is a prerequisite to estimate flow rates and pressure losses.

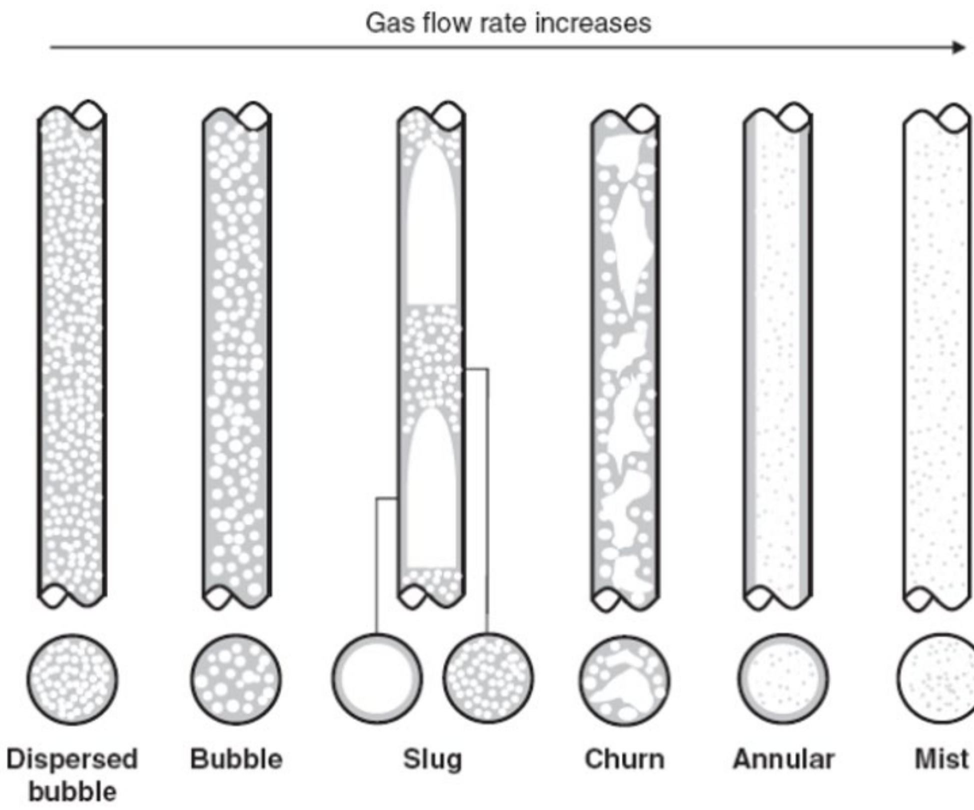

Figure 2.8 – Flow patterns for two-phase flow (Al-Safran and Brill, 2017).

Equation 2.24 describes the behavior of pressure loss, denoted as $\frac{dP}{dL}$, in pipe flow. It is derived from the momentum balance given by the Navier-Stokes equation.

$$\frac{dP}{dL} = \left.\frac{dP}{dz}\right|_{\text{gravity}} + \left.\frac{dP}{dL}\right|_{\text{friction}} + \left.\frac{dP}{dL}\right|_{\text{inertial}} \qquad \textbf{Equation 2.24}$$

An important point regarding this term is that the density of the fluids that will be produced will have a significant impact on the pressure loss. This is especially important, for example, when the water injected by injection wells reaches the producer and the percentage of water produced increases significantly. Therefore, as the density of water is generally higher than that of oil, a greater pressure loss results from this term. Another important scenario is when there is the production of high fractions of gas. The gravity term is also affected by the flow direction. If the flow is ascending, the gravity has a negative contribution.

The second term of the equation represents friction losses. As the fluid flows through the production system, energy is transferred to overcome the resistance to movement caused by the roughness of the walls and the viscosity of the fluid. This loss of energy results in a decrease in pressure throughout the flow. The magnitude of friction losses depends on several factors, such as the diameter of the pipe, the flow regime (laminar or turbulent), and flow velocity. In the case of multiphase flow, friction losses take on an even more complex role due to the presence of different phases, interacting with each other. The interaction between the phases can result in different flow regimes, as shown in Figure 2.8, such as bubble flow, slug flow, churn flow (turbulent flow with dispersed bubbles) and annular flow (annular flow) (Yadav, 2009).

The third term in Equation 2.24 is the inertial term. This term considers the acceleration of the fluid along the pipe. This term is particularly important in scenarios where there are sudden variations in speed or changes in flow direction, such as bends or deviations in pipes. According to Al-Safran and Brill (2017) this term can be neglected if there is no significant variation in momentum variation through the control volume (i.e. constant velocities and densities). According to the authors, the acceleration term is important at low pressure systems (<100 psi), which are rarely found in oil production systems. Thus, Equation 2.24 can be presented in the form of Equation 2.25.

$$\frac{\mathrm{d}p}{\mathrm{dL}} = -\frac{f_n \rho_n v_m^2}{2\mathrm{d}} - \rho_n g \sin\,\theta \qquad \textbf{Equation 2.25}$$

2.5 Nodal Analysis

The bottom hole pressure plays a crucial role in production. This is because a higher bottom hole pressure results in a more intense flow from the reservoir to the well. Conversely, a lower bottom hole pressure means less energy is available to lift the fluid to the surface. This condition generates opposing effects on the flow rate plots for the reservoir and the well. One method to enhance well production, considering both reservoir and column conditions, is through nodal analysis. The primary objective is to determine an operating point that optimizes and stabilizes production. The node can be placed at any point in the system but is generally considered to be at the bottom of the well (Jansen, 2017)

Thus, the flow performance curves in the production column are compared (OPR - *Outflow Performance Relationship*) with the reservoir production curves (IPR - *Inflow Performance Relationship*) (Zhou et al., 2016). Figure 2.9 shows the operational point, determined by the intersection of the IPR and OPR curves.

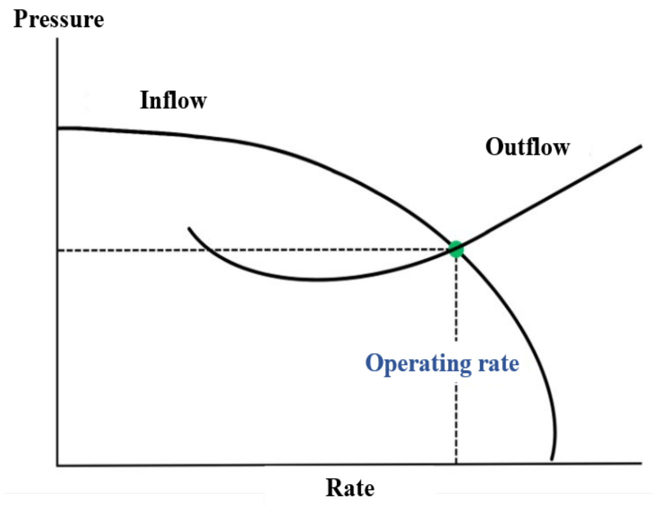

Figure 2.9 – Operational point between IPR and OPR (Lea and Rowlan, 2019).

2.5.1 Factors Affecting IPR and OPR Curves

The IPR curve is related to the flow conditions coming from the reservoir. Thus, changes in reservoir conditions, including depletion, formation damage, alterations in reservoir fluid characteristics, and changes in permeability, can impact the IPR curves. On the other hand, OPR curves are influenced by column conditions. For example, changes in friction factor, fractions of flowing fluids, flow pattern in the well, as well as the application of artificial lift techniques.

An important point to note is that these mentioned alteration processes are quite common throughout the productive life of the well, so the operating point should be reassessed when conditions in the reservoir or well vary.

2.6 Production System and Reservoir Integration (Integrated Models – IM)

Reservoir simulations, usually performed in commercial software, consider fluid flow within the porous medium, treating wells as sources or sinks located in specific simulation grid cells. However, analyzing total production through porous medium simulation alone cannot capture important effects that occur during fluid lifting in the well and flow through flowlines, pipelines, and platform facilities. Moreover, it is essential to remember that both well and reservoir conditions can be significantly altered due to the injection and production of various fluids. How previously discussed, this alteration implies changes in the IPR and OPR curves, thus altering optimal operating points. Therefore, it is crucial to consider flow conditions in each well and in the production system, reflecting them in the boundary conditions of the porous medium simulation. Integrating these two domains (production systems and reservoirs) is a challenging task given the substantial disparities in their temporal and spatial scales.

Integration can be achieved using various methodologies, including decoupled, explicit, and implicit approaches.

The implicit methodology employs a single simulator for reservoir and production system simulations, which offers greater flexibility regarding the number of projects and scenarios but demands higher computational resources.

The explicit methodology combines multiple simulators through a coupling program for data exchange, thus providing flexibility but potentially lacking consistency in physical properties and facing convergence challenges due to differences.

The decoupled methodology involves data exchange through pre-generated tables or files from the production system. While it limits the number of projects and planning scenarios due to modeling limitations, it is traditionally used in the industry and offers faster execution compared to other approaches presented (Cao et al., 2015; Hiebert et al., 2011).

3 LITERATURE REVIEW

This chapter aims to provide a literature review on polymer injection and integrated reservoir-production systems models, with focus on the heavy oil scenarios.

3.1 Polymer Injection

Several works in the literature report the effectiveness of polymer injection in heavy oil reservoirs. Li et al. (2014) presented an analysis of laboratory experiments, development models, and polymer injection simulation studies in a heavy oil reservoir with active aquifer influxes. The authors concluded that polymer injection is a viable technology for such reservoirs, even in the presence of highly unfavorable mobility ratios and significant aquifer influxes.

Lamas et al. (2018) discussed the selection of an oil field production strategy, considering water flooding, ideal polymer injection, and polymer flooding with a focus on four key polymer properties: retention, viscoelasticity, salinity, and degradation. They analyzed these strategies probabilistically and found that degradation has the most significant impact on NPV (net present value), followed by salinity, viscoelasticity, and retention. Comparisons revealed that strategies involving water and ideal polymer serve as performance limits for the field, which provides valuable insights even before precise polymer data is available.

Botechia et al. (2019) investigated optimizing polymer injection strategies to mitigate water-oil mobility issues applied to offshore heavy oil fields. They explored alternating water-polymer cycles, assessing parameters like polymer bank duration and start date. They found that reducing the cycle period positively impacts stable injection flow at higher levels, preventing a reduction in oil production due to pressure depletion. Additionally, the authors noted that it is essential to start the cycles in the early years following the initiation of water flooding.

Gao (2011) conducted two pilot tests in the Bohai field to evaluate the use of polymers as EOR strategy. The first test was conducted on a single well, while the second followed the five-spot pattern. Both tests yielded significant results, with an increase in oil production and a reduction in water cut. The reservoir in the Bohai region has an average depth between 1,300 and 1,600 meters, with porosity ranging between 28% and 35%, an average permeability of 2,600 mD, and an average temperature of 65°C. The average spacing between wells is 370 meters. The single-well pilot test lasted about 500 days and resulted in a reduction in water cut from 95% to 54%, in addition to producing an additional 25,000 m3 of oil. Based on the success of this treatment, polymer injection began in four injection wells and six production wells since 2005. Each well produced about 17,700 m3 of additional oil, and water cut was reduced by 10%. By 2010, 53 polymer injection operations had been carried out, resulting in a total oil increase of about 636,000 m3.

Lamas et al. (2021) evaluated three model-based approaches to increase productivity in mature oil fields. The first approach involved a standard water injection strategy, while the second approach focused on using an aqueous polymer solution as the injection fluid. The third approach included converting injector wells to producers and vice versa, strategically targeting remaining oil points. These methodologies proved to be economical and easily applicable, leading to higher oil recovery and NPV. The results highlight the potential to revitalize mature oil fields and maximize their production potential.

The efficiency of polymer injection is generally influenced by various factors, including the injection scheme, the timing of injection relative to well production history, and effects related to the porous medium, such as reservoir heterogeneities, alteration of relative permeability curves, polymer adsorption or polymer degradation due to shear in pore (Silveira et al., 2024).

Additionally, for operational parameters and porous media, the well completion and production systems can greatly influence the production recovery. The case is more complex for reservoir containing multiple interconnected producing wells in a production system. The operational control decisions made for each well can affect the overall recovery efficiency in the field. This means that well variables, typically boundary conditions in reservoir simulations, can modify how the polymer front is distributed and, consequently, sweep efficiency (Lake, 2006; Zhao et al., 2021).

3.2 Integration Between Reservoir and Production System

Su et al. (2016), studied an integrated asset model for a large offshore Abu Dhabi oil field with two subfields with over 600 production and injection strings. One interesting conclusion the authors reached was that developing and maintaining an integrated asset model is resource-intensive and requires tasks like converting reservoir models, troubleshooting software issues, and adapting workflows. Updates to historical data or drilling schedules further complicate maintenance, often requiring recalibrations and model adjustments. Therefore, in mature giant fields, it may be more practical to use non-integrated models for evaluations or sensitivity analyses that involve limited changes to drilling schedules and updating the model annually or biannually to manage operational complexities.

Several works in the literature investigate the simulations using an integrated approach. Rotondi et al. (2008) emphasized the importance of integration and revised several aspects of the implementation. Ghorayeb et al. (2003) highlighted the complexity of the current oil production scenario, involving multiple reservoirs shared among various platforms, operational constraints, the blending of fluids with distinct properties, and offshore production systems, which demand a more precise integration between reservoir and production system modeling.

Victorino et al. (2018) conducted integrated and decoupled analyses using the UNISIMI-D benchmark case. Their findings suggest that, while a reservoir may have the capacity to produce at a specific flow rate, real production outcomes may deviate from initial forecasts. Moreover, the study identified that future modifications in the production system could have a critical impact in sustaining or enhancing production levels, ultimately leading to improved financial returns.

Notably, the integrated analysis provided more realistic insights into field production, offering a comprehensive evaluation that combined considerations of oil production and financial performance. It is essential to emphasize that financial analysis, particularly through the NPV approach, as used by Victorino et al. (2018), plays one essential role in evaluating the economic viability of Enhanced Oil Recovery (EOR) strategies. This significance is underscored when incorporating chemical agents like polymers or surfactants into the EOR process. NPV considers the initial capital investments necessary for implementing these strategies, ongoing operational expenses, and the expected revenues derived from the augmented oil production achieved through EOR efforts. Through the application of a discount rate, NPV provides an assessment of the future cash flows in present-day terms.

Victorino et al. (2021) presented in their work an integrated simulation of the production system, reservoir, and manifolds to assess the impact on final oil production. The production strategy analysis methodology was evaluated in five sequential stages, which include well allocation (producers and injectors), determination of the optimal number of wells for production, assessment of manifold usage and allocation, conducting sensitivity analysis on the collection system diameters and platform allocation. Each stage builds upon the best result from the previous stage. The results highlighted the importance of each stage in forming the production strategy and proposed an ideal configuration to ensure satisfactory financial return.

The analysis also identifies crucial stages for optimizing complex scenarios with reduced discontinuities, convergence issues, and computational effort.

Victorino et al. (2022) evaluated the influence of parameters in an oil production strategy in a carbonate reservoir and its impact on financial and production yields. Two approaches were considered: a non-integrated (NI) one with fixed conditions for the well and collector system, and an integrated (I) one with variable conditions. The analysis involved several steps to determine the best extraction strategy for both systems based on net present value. The results showed that simplification (NI) could affect financial yield but integrating the NI system resulted in considerable financial and production differences. Optimizing the integrated model can be beneficial in simplified systems, as key aspects of financial return are related to reservoir model behavior.

Hohendorff Filho and Schiozer, (2022b) proposed effective integrated optimization approaches to develop an optimized water injection scheme for sandstone and carbonate reservoirs, using two approaches, called “A” and “B”. In approach "A", integration occurs at an intermediate stage of the optimization process. In approach "B", integration is present in all optimization stages. Both suggested methodologies for optimizing the production system showed efficiency in reaching the final production strategy, showing optimal results regarding the number and positioning of wells in different periods. The analysis revealed a significant difference in production forecasts, but similar results in the production strategy and net present value of the optimized project, emphasizing the importance of its inclusion in optimization processes.

3.3 ESP Application in Heavy Oil Fields

This section aims to highlight the main works used to modeling the production system for the IM1. It is important to highlight that the development of this work is for a new field and for starting point the references of analogs reservoirs are fundamental.

The development of heavy oil reservoirs presents significant challenges, primarily due to the inherent physical properties of heavy oil, such as its high viscosity and density. These characteristics significantly increase the pressure required to transport the oil to surface facilities. In this context, Electric Submersible Pumps (ESPs) have become an indispensable technology in heavy oil production, serving as a key method of artificial lift. As example, Castro et al. (2019) highlight that the artificial lift strategy using ESP was fundamental to achievement of 104,000 STB daily oil production in Peregrino field, supported by two platforms, integrating production and drilling capabilities.

In the study of Beall et al. (2011), an integrated approach combining ESPs and downhole flowmeters was investigated for heavy oil production in Brazil's offshore field. The research focused on validating and analyzing the allocation performance of downhole flowmeters alongside ESPs under varying conditions of well behavior, including production rates and bottom-hole pressure. Authors reported the utilization of 12 and 17 pump stages. Initial testing, covering flow rates from 500 to 30,000 barrels per day and oil viscosities up to 360 cP, aimed to benchmark the combined performance of ESPs and flowmeters. An iterative method for adjusting the flowmeter discharge coefficient based on measured fluid properties was developed, improving measurement accuracy. The study confirmed the ESP and flowmeter integration's efficacy for heavy oil allocation, with flowrate deviations within ±5% for ESPs.

Olsen et al. (2012), as extension of the previous work (Beall et al., 2011; Olsen et al., 2011), conducted a comprehensive evaluation of ESPs for flow allocation in the heavy oil field, off the coast of Brazil. Recognizing the limitations of traditional flow allocation devices in offshore settings, particularly regarding space and accuracy with heavy oils, the study sought an efficient alternative. Utilizing the known models of ESP systems, well, and fluid parameters, the research team embarked on calibrating three submersible pump types under a range of operational conditions reflective of the field's requirements. This calibration was essential for refining the ESP flow allocation method, aiming to enhance its accuracy for both head and brake horsepower measurements. The findings, corroborated by a comparison with the FPSO's fiscal meter, revealed deviations within the 5% threshold mandated by Brazilian regulations. The study not only confirmed the viability of using ESPs and downhole Venturi flow meters for heavy oil production allocation but also indicated that the number of pump stages (specifically, tests with 6 and 12 stages) had negligible impact on performance in viscous liquids. This work lays the groundwork for more precise and space-efficient flow allocation methods in offshore heavy oil production.

Kristoffersen et al. (2017) presented a model-based production optimization approach for the Peregrino Field, focusing on determining optimal ESP frequency settings for each well to maximize oil production amid water injection constraints. Authors reports the utilization of ESPs with 12 and 17 stages. Employing a Mixed-Integer Linear Problem (MILP) formulation, the methodology integrated piecewise linear tables derived from a commercial simulator to accurately represent well performances. According to authors, this approach facilitated rapid optimization conducive to real-time application, effectively managing multiple operational constraints and ensuring global optimality.

Pastre et al. (2022) delved into the performance of Electric Submersible Pumps (ESPs) in high viscosity oil conditions, specifically within the Peregrino field. Recognizing the limitations of traditional correlations used for ESPs in such environments, the study utilized single-phase and multiphase tests conducted alongside a decade of operational data from Peregrino to analyze ESP performance, emulsion production, and phase inversion phenomena. Configurations of 6 up to 9 stages were evaluated, testing across 17 different viscosities and 6 rotational speeds. The research uncovered that traditional models do not accurately predict ESP behavior under high viscosity, leading to operational inefficiencies and equipment failures.

From the literature review conducted, it is observed that the studies typically utilize a range of 8 to 15 stages in ESP systems for heavy oil fields with characteristics similar to those investigated in this work.

4 METHODOLOGY

The methodology of this work is based on six steps:

I. Select the production strategy, referred to as integrated model 1 (IM1), using information from literature.
II. Compare IM1 with the non-integrated model (NIM).
III. Adapt the production system to reach similar values to the target BHP by adjusting the pump stages to achieve oil production values close to the NIM (IM2).
IV. Evaluate the impact of polymer injections in IM2.
V. Determine the optimal polymer concentration for each scenario under maximum oil production and maximum NPV.
VI. Implement an alternative NIM approach with a revised BHP to get similar results of the integrated solution (NIMr).

4.1 Reservoir and Production System Integration

To integrate the reservoir with production system and evaluate the impact of integration compared with the non-integrated case, it was followed four main steps: (1) model the production system; (2) generate the vertical flow performance table (VFPs); (3) integrate it with reservoir simulation; (4) implement the polymer injection for an integrated system and comparison with non-integrated case.

Figure 4.1 shows the general workflow of the work. It was modeled the production system based on data found in the literature and this first model is called IM1.

This model is compared with the non-integrated model, which serves as the target model, in terms of production values. This model is called NIM. If the production results obtained with the IM1 model are lower than those of the NIM, it was created the IM2 model, in which adjustments are made to the production system to achieve the NIM.

After obtaining these results for IM2, it was carried out an economic evaluation for all cases obtained. Figure 4.2 shows the flowchart of the integrated simulations methodology, where STM means a mixed number of stages; ST20 is 20 stages; ST37 is 37 stages; ST50 is 50 stages; and ST80 is 80 stages.

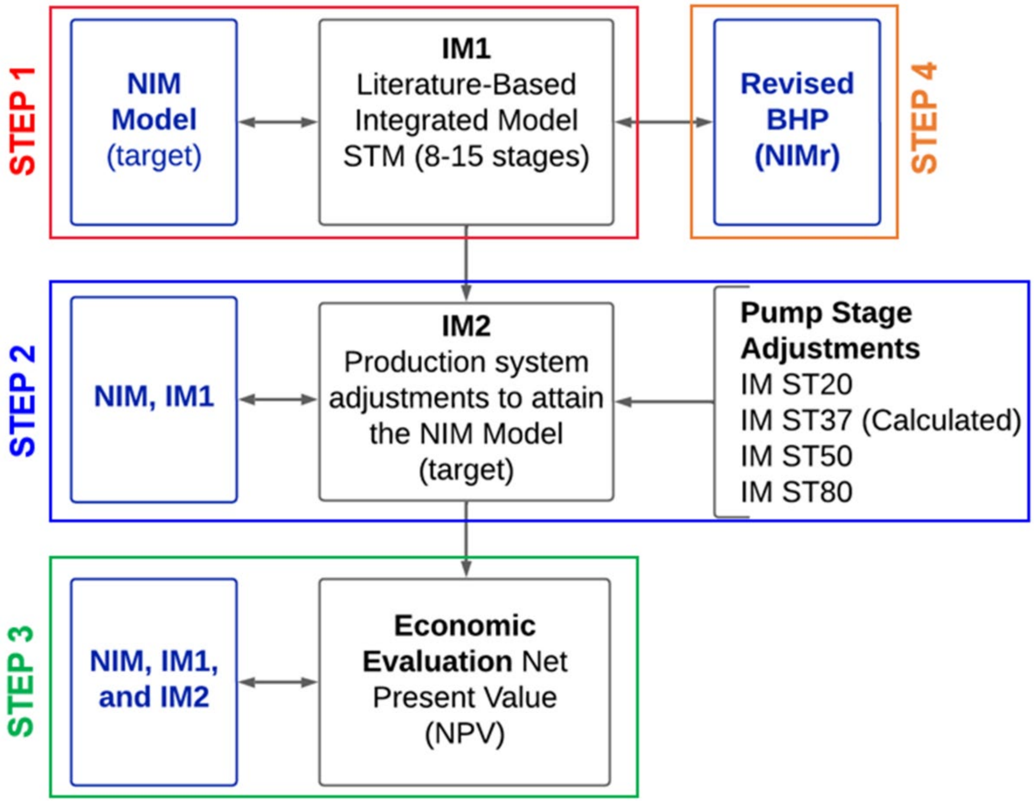

Figure 4.1 – General workflow.

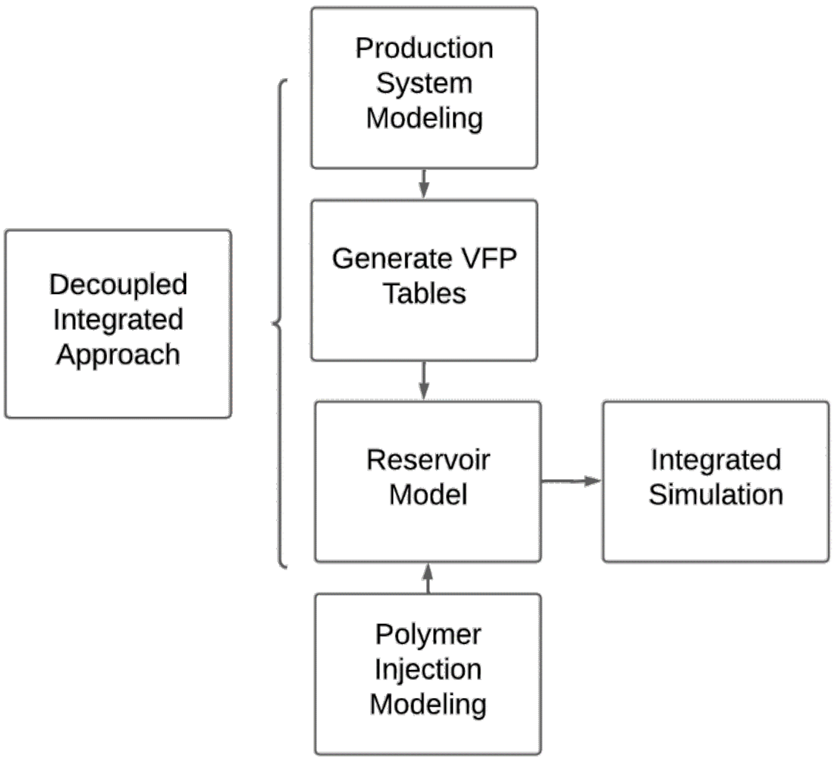

Figure 4.2 – Methodology flowchart for integrated simulations.

4.2 Non-Integrated Model Based on a Revised BHP (NIMr)

In this methodology, it is estimated a Revised BHP value for non-integrated models (NIMr). This NIMr ensures oil production compatibility between NIM with IM. The main objective of this approach is simplifying the process by using a single software to capture the effects of integration, resulting in reduced computational time.

To obtain the NIMr a sensitivity analysis of the BHP within the NIM is conducted. Starting with the minimal BHP pressure of the NIM, it is iteratively adjusting the minimum BHP, starting to be adding pressure increments, and comparing the results of oil production with the IM. The pressure increments are fine-tune until achieving the smallest difference in final production values within the IM. This last BHP value obtained is called the Revised BHP. It is repeated this procedure for various polymer scenarios, including waterflooding and polymer concentrations, obtaining a NIMr for each scenario.

5 APPLICATION

5.1 Production System Flow Simulation

The model utilized in this study includes riser, flowline, production columns, and completion equipment for production wells. The water depth is approximately 120 m.

Figure 5.1 shows an example of a producer well. All producer wells were set up with submersible electric centrifugal pumps of the HC20000 type, with 0.173 m (6.8 in), operating at base frequency of 60Hz. These pumps are designed to handle operational flow rates ranging from 1271.89 to 3179.97 m³/day (8,000 to 20,000 bbl/day). The number of stages was evaluated under different scenarios, according to the base case (spanning from 8 to 15 stages) (Olsen et al., 2011; Olsen et al., 2012; Pastre et al., 2022), and cases with 20, 37, 50, and 80 stages.

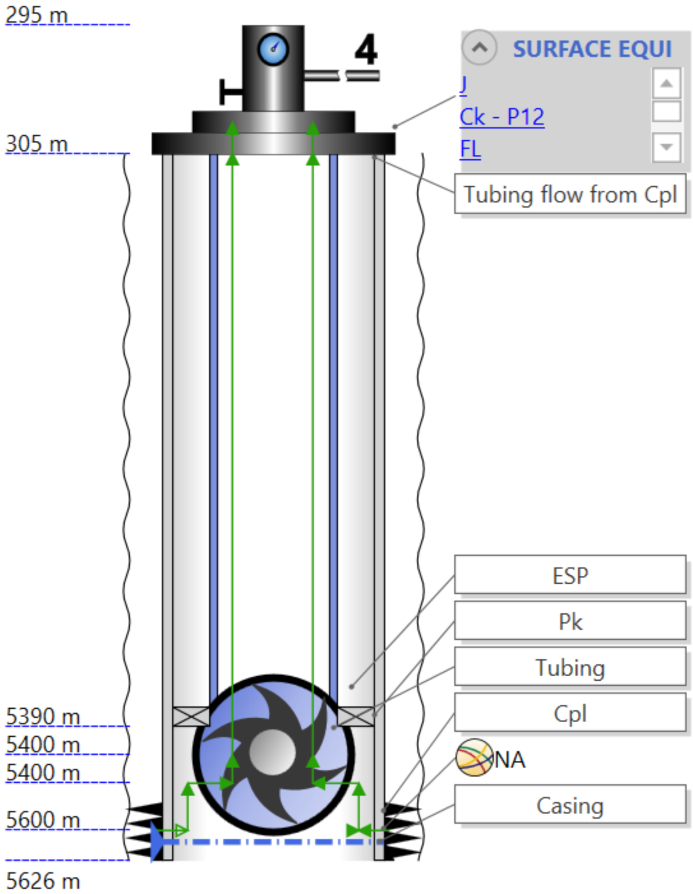

Figure 5.1 - Example of a producer well equipped with an ESP.

Figure 5.2 presents the characteristic performance curve of a Baker HC20000 pump with 37 stages, operating at 3,500 RPM and 60 Hz.

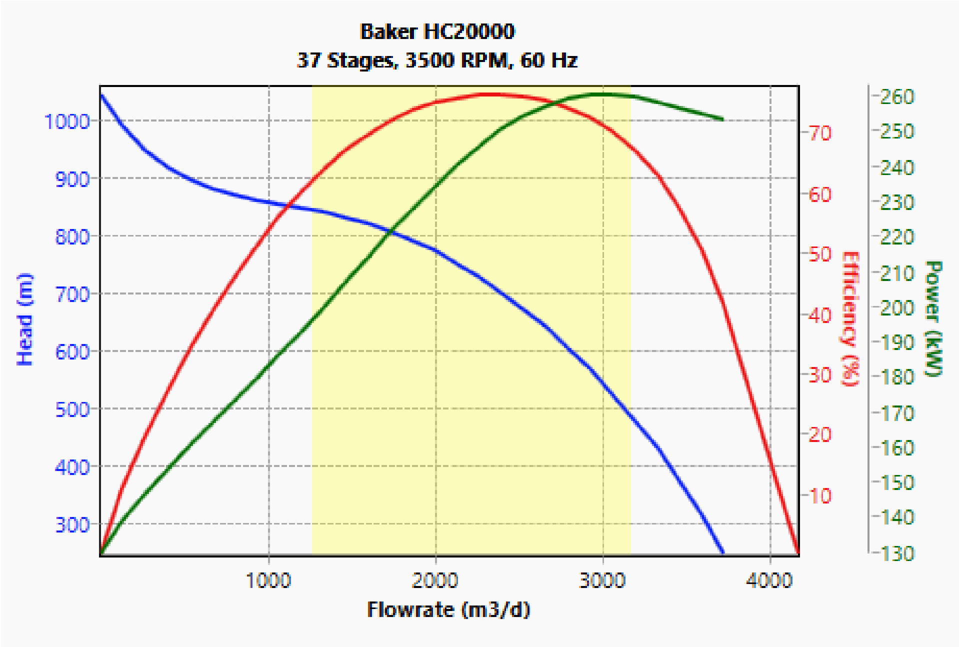

Figure 5.2 - Performance characteristics of the Baker HC20000 Pump

Under these conditions, the operational range is maintained between 1,000 and 3,100 m³/day. The maximum efficiency, achieved at 2,500 m³/day, is approximately 75%, with a head of 750 m and a power requirement of 250 kW.

One important aspect is that the performance data showcased in Figure 5.2 are specifically based on a pump configuration of 37 stages, operating at a frequency of 60 Hz. Any variation in the electrical frequency not only alters the pump's rotational speed but also significantly influences its efficiency, head, flow rate, and power requirements. Similarly, adjustments in the number of stages directly affect the pump’s ability to generate head, thereby impacting its overall performance including efficiency and operational capacity.

The production system consists of four producer wells. The production flows from these wells, which are interconnected through a manifold in the platform, which in turn further connects to flow lines until a phase separator.

The wells were equipped with casing that had an outer diameter of 0.244 m (9.625 in) and an inner diameter of 0.225 m (8.835 in) and a roughness of 0.025 mm (0.001 in). The tubing featured an outer diameter of 0.1397 m (5.5 in) and an inner diameter of 0.1242 m (4.892 in). The temperature at the wellhead was considered 60°F (15.6°C) across all wells. For the tubulars, the well pressure drop was calculated using the revised Beggs and Brill correlation for multiphase flow (Beggs and Brill, 1973).

Table 5.1 provides the operational limits for both producers and injectors used in the NIM. These conditions have been specified by the field operator and are directly linked to the operational limits of equipment, as well as to prevent issues related to sand production resulting from excessive flow rates. For the IM, the same limits flow rates were used, but no specifications were set for the minimum BHP.

Table 5.1 - Wells operational parameters.

Producers		Injectors	
Max. liquid production	2,500 m³/day	Max. rate injection	3,000 m³/day
Minimum BHP	125 bar	Maximum BHP	220 bar

After the PS was modeled, the next step involved deriving the IPR for each well, considering temperature, liquid flow rates, and water cut (WC) generating the VFP (Vertical Flow Performance) tables in the PIPESIM ^{TM}.

VFP plots are illustrated in Figure 5.3. VFP allows to capture the dynamics of fluid flow in the well.

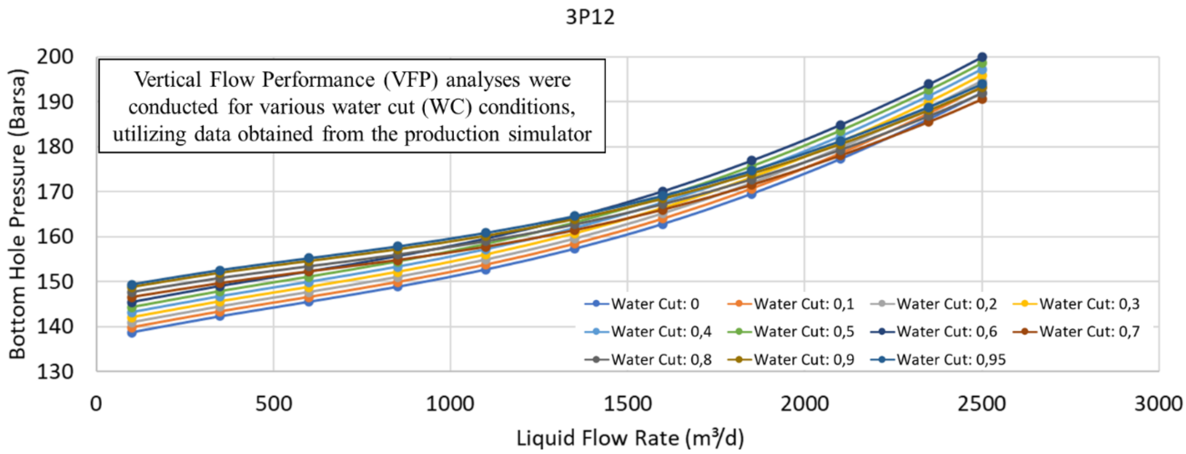

Figure 5.3 – Example of decoupled integration implementation - Vertical Flow Performance Plots.

5.2 Field Description

This study used a reservoir model, illustrated in Figure 5.4, which was constructed representing a specific region of a real offshore sandstone heavy oil field. In the following sections, it is provided an overview of the reservoir and production system characteristics.

The reservoir simulation model, referred to as EPIC001, utilizes a grid configuration with cell dimensions of 100m x 100m in the x and y directions and variable cell thickness (averaging at approximately 1.94m) in the z direction. This grid comprises a total of 93,810 cells arranged in a three-dimensional space with dimensions of 30 cells in the X direction, 53 cells in the Y direction, and 59 cells in the Z direction. The reservoir's initial conditions include pressure of 223 bar and temperature of 82°C.

The simulation model features seven wells, including four producers and three injectors, and initial testing was conducted using waterflooding as the secondary recovery method.

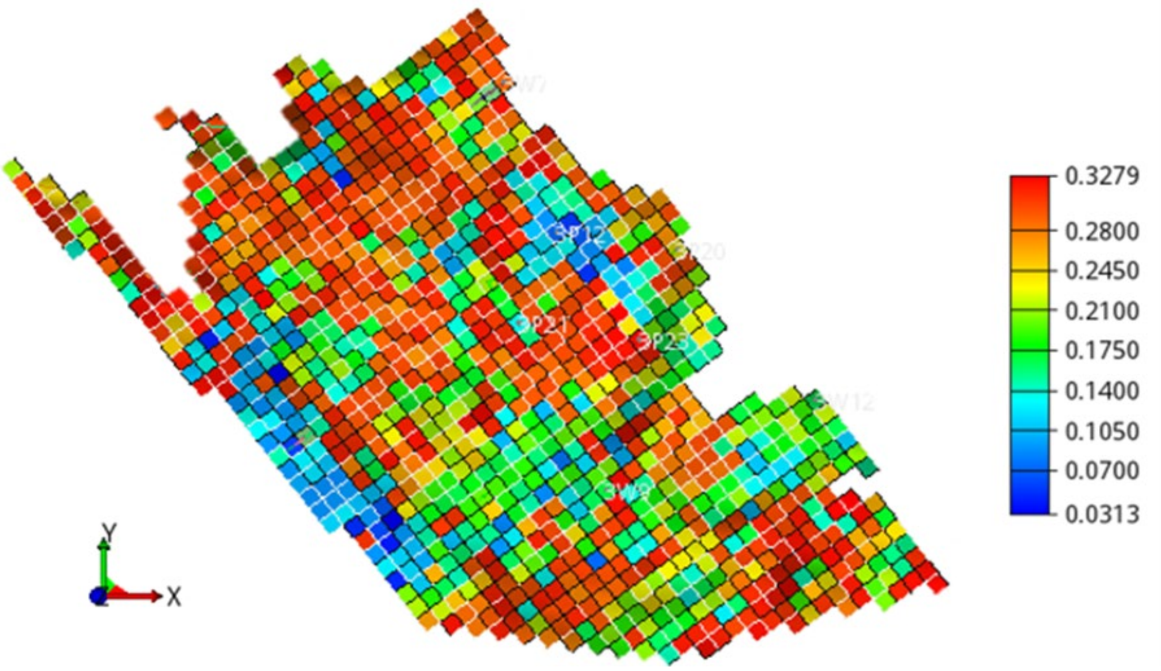

Figure 5.4 – EPIC001 porosity map in the layer k=12.

A summary of the primary reservoir parameters can be found in Table 5.2. Within the reservoir fluid, a Black-oil model was used.

Table 5.2 - Reservoir simulation parameters.

Parameter	Min	Max	Average
Average permeability (mD)	0 (x and y) 0 (z)	8888 (x and y) 6221 (z)	3458 (x and y) 2413 (z)
Average Porosity (%)	3	31	24
Depth (m)	1933	2332	2138
Temperature (°C)			82
Initial pressure (bar)	202	236	220
Oil in place (m^3)			$89.8x10^6$
Oil viscosity (cP)	30.9	32.6	31.8
Initial oil saturation (%)	5	91	63

5.3 Polymer Injection Configuration

Simulations were performed using the IM and NIM approaches. For integration, the keyword VFPROD was used in the SCHEDULE section of ECLIPSE to include the VFP tables generated in production simulator, PIPESIM ™. Polymer concentrations were simulated in concentrations of 0.1 up to 2.49 kg/m^3, using the keyword WPOLYMER to define the polymer concentration. The injection rate was set using the keyword WELTARG with an injection rate of 3,000 m^3/day. The polymer injection in all the cases was implemented according to Figure 5.5, with continuous water injection in the first five years followed by 15 years of polymer injection.

Time (years)	1	2	3	4	5	6	7	8	9	10	11	12	13	14	15	16	17	18	19	20
Recovery stategy	Water Injection					Polymer Injection														

25% of time

75% of time

Figure 5.5 – Polymer injection scheme.

The polymer modeled corresponds to the viscosity of Hydrolyzed Polyacrylamide HPAM, with molecular weight 12-16 MDa (Silveira et al., 2024). It is worth mentioning that an ideal polymer solution was modeled, that is, effects such as adsorption and degradation were not considered. The value of viscosity of the mixture at concentration of 2.49 kg/m^3 was around 20 cP. The viscosity of polymer solution was implemented as linear correlation for the other concentrations.

5.4 Integrated Simulation Scenarios

In this study, the methodology comprised four distinct steps. Initially, it was constructed the PS, referred to as IM1, using data sourced from the literature (Beall et al., 2011; Castro et al., 2019; Kristoffersen et al., 2017; Olsen et al., 2012, 2011; Pastre et al., 2022). In the IM1, it was used a mixed configuration for the ESP, called STM (spanning from 8 to 15 stages). It was compared the results with the NIM.

Subsequently, in the second phase, it was refined the production system by adjusting the pump stages (designated as IM2) to attain the production targets of the NIM. For this, it was estimated the number of stages for the pump, which in the IM1 model was 8 to 15 (STM). This estimation was made through correlations and with the PIPESIM tool, reaching a value of 37, which it was called ST37. In addition to this estimated value, it was evaluated one scenario with a number of stages below, the ST20 and two scenarios with higher numbers of stages, the ST50 and ST80 for comparison purposes.

The modeling of wells and production system was made using PIPESIM ™. VFP tables were generated for each well considering their geometry and the ranges of flow rate, Bottom Hole Pressure (BHP), Water Cut (WC), temperature, and pump frequency. After these were generated, the VFP tables were implemented in ECLIPSE™, and the simulation performed in integrated mode.

Following this, it was assessed the impact of the preceding steps before incorporating considerations related to water and polymer flooding. Ultimately, it was conducted an analysis to determine the optimal polymer concentration for each scenario.

5.5 Economic Evaluation

For economic assessment, NPV approach was used as an indicator for profitability. For platform cost, Equation 5.1 was employed, where Inv_{plat} represents the investment in the platform (x10^6 USD), C_{Pl} is the liquid processing capacity (x10^3 m^3/USD), C_{Po} is the oil processing capacity (x10^3 m^3/USD), C_{Pw} is the water processing capacity (x10^3 m^3/USD), C_{iw} is the water injection capacity (x10^3 m^3/USD), and C_{nw} is the number of wells capacity.

$$Inv_{plat} = 417 + 3.15 \times C_{Pl} + 12.2 \times C_{Po} + 3.15 \times C_{Pw} + 3.15 \times C_{iw} + 0.1 \times C_{nw}$$ **Equation 5.1**

Equation 5.2 shows the NPV calculation. Here, NCF$_j$ represents the net cash at a specific time "j". N$_t$ is the total number of time periods, "i" is the tax rate, and t$_j$ is the period of the analysis.

$$\mathrm{NPV} = \sum_{j=1}^{N_t} \frac{\mathrm{NCF}_j}{(1+i)^{t_j}}$$ **Equation 5.2**

The net cash flow for each period (NCF) is calculated using Equation 5.3, which considers various financial factors including R (gross revenue from oil), Roy (total royalties), ST (total social taxes), OC (operational costs of production), T (corporate tax rate), Inv (investment in equipment and facilities), and AC (abandonment cost).

$$\mathrm{NCF} = [(R - \mathrm{Roy} - \mathrm{ST} - \mathrm{OC}) \cdot (1 - T)] - \mathrm{Inv} - \mathrm{AC}$$ **Equation 5.3**

Table 5.3 provides the values used in the economic model. It was also considered a corporate tax rate of 34%, a social tax rate of 9.25%, and royalties at 10% charged over gross revenue.

It is important to clarify that the NPV analysis conducted herein does not incorporate the increased capital expenditure and energy costs associated with a greater number of pump stages, simulated in IM1 and IM2.

Table 5.3 - Parameters used in the economic model.

Variable/parameter	Value	Unit
Discount rate	9.0	%
Oil price	314.5	USD/m^3
Operational fixed cost	1.0	10^6
Oil production cost	62.9	USD/ m^3
Water production cost	6.29	USD/ m^3
Polymer mixture production cost	4.0	USD/kg
Polymer powder production cost	3.0	USD/kg
Water injection cost	6.29	USD/m^3
Polymer injection cost	6.0	USD/kg
Drilling and completion of horizontal well (fixed cost)	60.0	10^6 USD
Connection of well (well-platform)	13.3	10^6 USD
Drilling and completion of vertical well	14.0	10^6 USD
Recompletion of horizontal well	3.0	10^6 USD
Recompletion of vertical well	3.0	10^6 USD
Well conversion	3.0	10^6 USD
Platform	Equation 5.1	10^6 USD
Abandonment cost	6.0	10^6 USD

Figure 5.6 presents the timeline of events for the field's production, starting in February 2020 with the start of simulations and well drilling operations and ending in 2042.

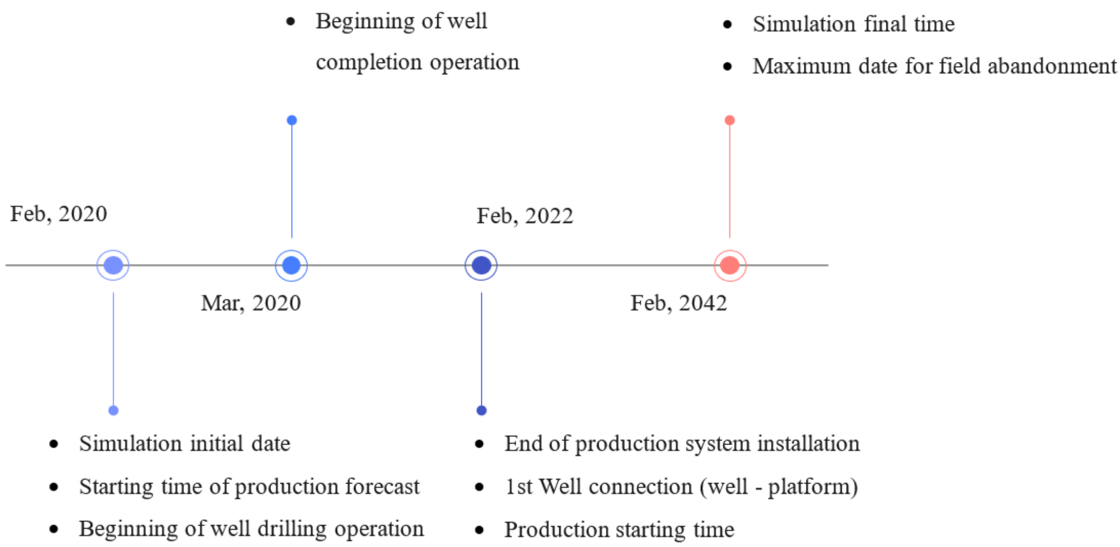

Figure 5.6 – Timeline of the main events.

5.6 Revised BHP Determination (example)

This section illustrates the methodology used to determine the Revised BHP and provides clarification on the approach used in NIMr. Before detailing the example for obtaining the Revised BHP, it is important to highlight key aspects related to BHP in numerical reservoir simulation.

The first point to consider is that BHP serves as a boundary condition in reservoir simulation. Typically, the constraints applied are a minimum BHP and a maximum flow rate, allowing the flow rate and pressure to operate within these limits under well's boundary conditions.

In the integrated case, the boundary conditions are not independent but are directly linked to well performance parameters, correlated in the VFP Tables, as explained in the integrated approach modeling sections, 2.6 and 5.1.

The NIMr approach aims to identify a minimum BHP value that accurately represents the production in the IM. This involves accounting for pressure losses in the production system, which typically results in the Revised BHP used in NIMr being higher than the BHP used in the NIM.

Table 5.4 provides an example from simulations conducted to determine the Revised BHP in the case of a polymer injection scenario with concentration of 2.49 kg/m^3. The initial step involved adding 40 bar to NIM (Run 1). This adjustment decreased the discrepancy between the NIM and IM1, though the difference remained significant (18%).

Table 5.4 - Results of sensitivity analysis simulations.

#Run	Pressure added (bar)	BHP Estimated (bar)	Total oil production (m³/day x 10^6)	Difference between NIM and IM1 (%)
1 - NIM	-	125 (NIM)	25.05	43%
2	+40.0	165.0	18.96	18%
3	+10.0	175.0	16.66	9%
4	+5.0	180.0	15.32	4%
5 – NIMr	+2.5	182.5	14.62	1%
6	+2.5	185.0	13.87	-2%
7	+2.5	187.5	12.41	-8%

Subsequent simulations involved incrementally increasing the pressure, aiming to minimize the difference between NIM and IM1. This fine-tuning continued until the difference neared zero. Ultimately, in Run 5, was achieved a minimal difference of 1% between NIM and IM1, this model was called NIMr. Additionally increasing the pressure above 182.5 bar does not further reduce the difference but instead increases it (Runs 6 and 7).

Figure 5.7 shows the oil production plots from the example provided, serving as a sensitivity analysis of BHPs for total oil production. The curves more closely align with the IM1 in subsequent runs, with the closest match occurring for 182.5 bar (Run 5).

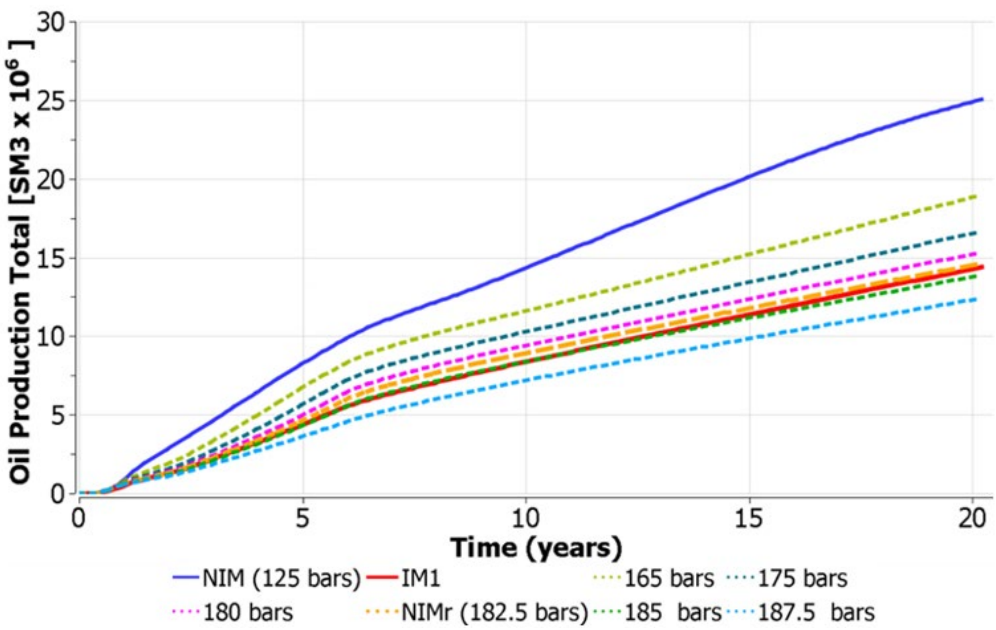

Figure 5.7 – Example of sensitivity analysis of BHPs for a polymer injection scenario.

The numerical simulations were performed on a virtual desktop infrastructure (VDI) configured with an Intel(R) Xeon(R) Gold 6144 CPU @ 3.50 GHz, equipped with 4 cores and 24.0 GB of RAM. The system operated on a 64-bit, x64-based architecture.

6 RESULTS AND DISCUSSION

In this chapter, it was presented the main results obtained based on the methodology and application scenarios outlined in Chapters 4 and 5.

6.1 Influence of Integration (IM1)

6.1.1 Waterflooding

Figure 6.1 presents a comparative analysis of total (cumulative) oil production between two scenarios: the base case, which involves water injection without integration, and the case with integration. Notably, the implementation of the production system led to a reduction in production of roughly 23%. This observation underscores the substantial influence of pressure loss on final oil production and emphasizes the critical role of accounting for the production system within the reservoir simulation process. It is important to note that the results obtained also suggest that the production system may be undersized. It could potentially be a consequence of inherent differences in the integrated approach to modeling.

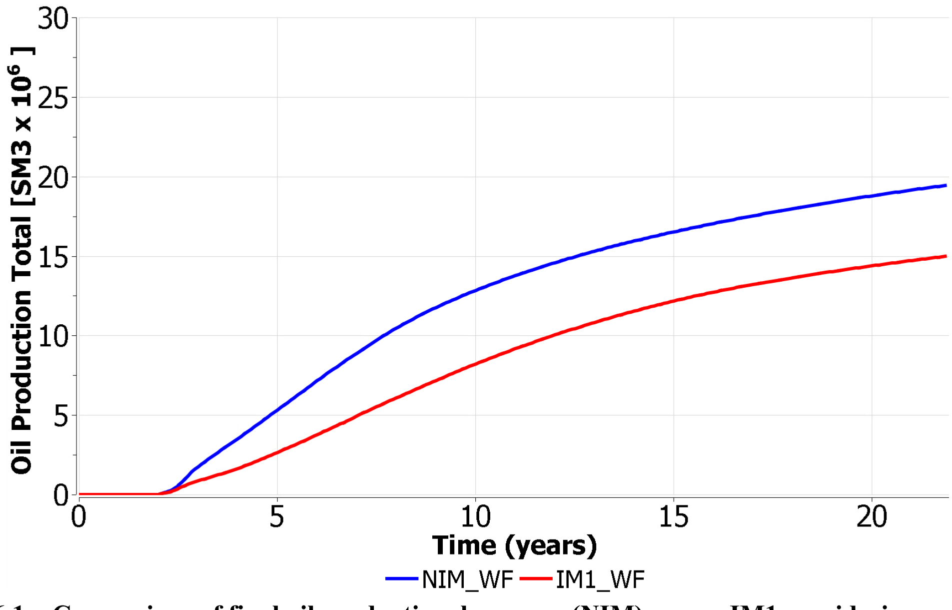

Figure 6.1 – Comparison of final oil production, base case (NIM) versus IM1 considering only water injection.

Figure 6.2 shows the BHPs for all producer wells. It is possible to observe a noticeable trend for the BHPs of all wells, when considering integration, which consistently exceeds the BHPs observed in the base case. Among these, well 21 (indicated by the red curve) exhibits the highest BHP, while Well 23 (represented by the blue curve) shows the lowest BHP.

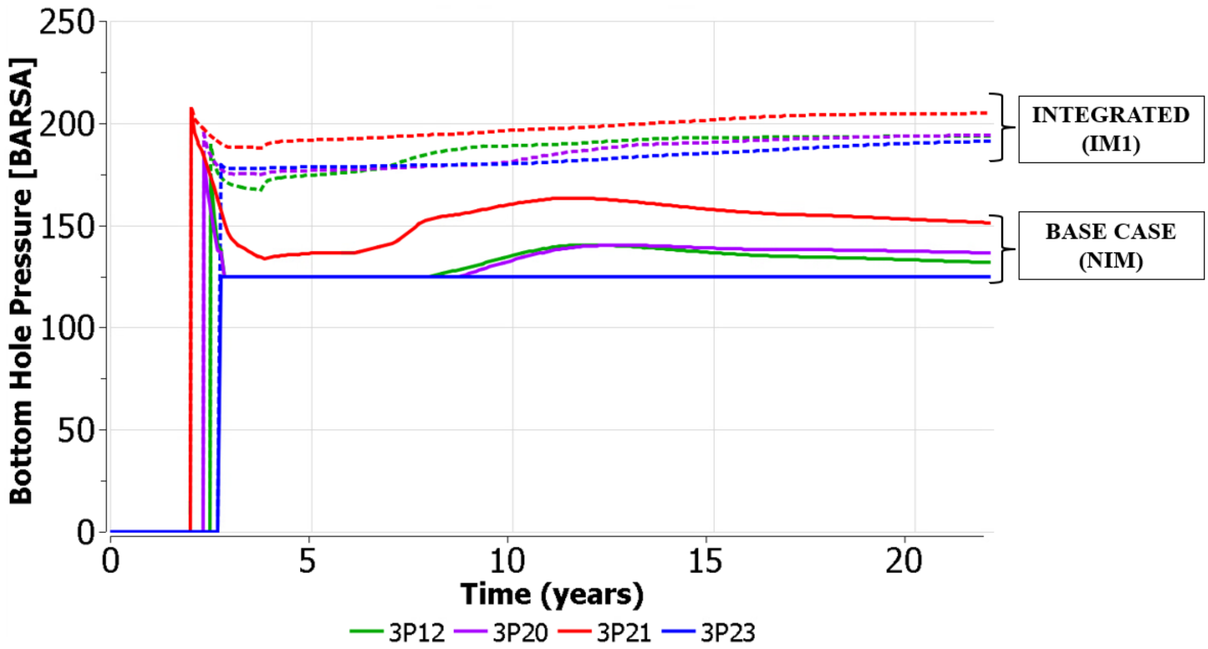

Figure 6.2 – Comparison of BHP, NIM versus IM1 for water injection.

Figure 6.3 presents the curves of the total amount of water produced in the water injection scenario for the NIM and IM1 cases. It is possible to observe that water only began to be produced from the seventh year for the NIM and eighth year for the IM1.

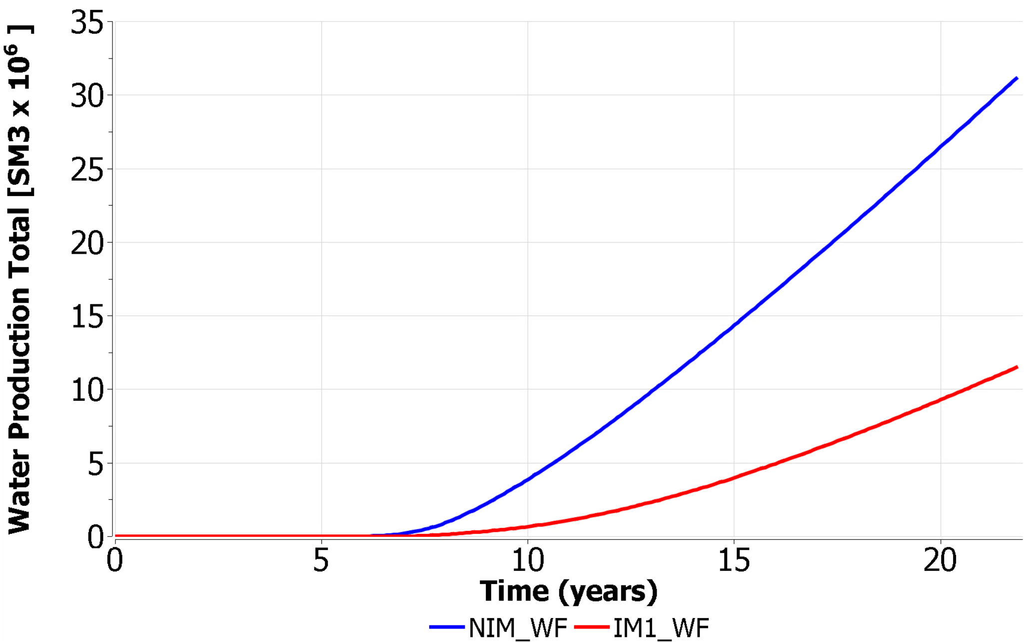

Figure 6.3 – Total water produced for waterflooding.

Coincidentally, Figure 6.4 shows that this is the same period in which oil flow begins to decrease for NIM and IM1. Additionally, total water production, in Figure 6.3, after 22 year was considerably lower for the NIM compared to IM1.

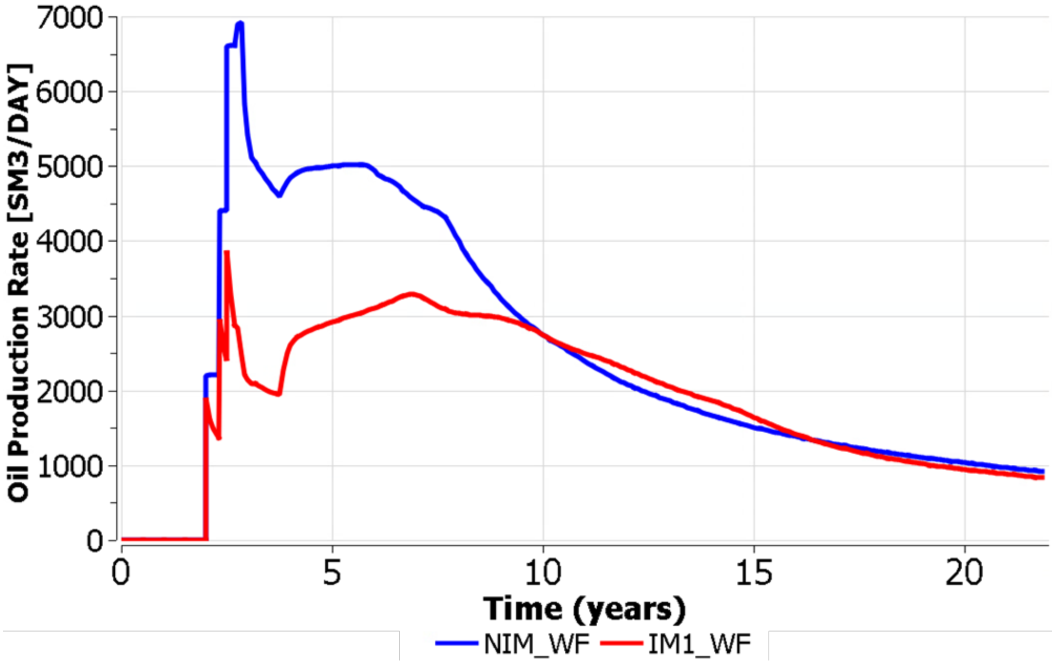

Figure 6.4 – Oil flowrate for waterflooding.

6.1.2 Polymer Flooding

Figure 6.5 illustrates the results of total oil production over time for polymer injection, comparing scenarios with and without integration. Specifically, it was employed a polymer concentration of 2.49 kg/m^3. It is evident that, like the observed effects in waterflooding injection, the integrated approach resulted in a reduction in oil production. Notably, this reduction is more significant when polymer injection was incorporated, resulting in a decrease of 41%. This discrepancy highlights the sensitivity of polymer injection to integration effects. The primary reason for this phenomenon can be attributed to the pressure drop introduced by the production system. Moreover, with polymer injection, the average pressure in reservoir also tended to increase. The pressure drops in reservoir, added to the increase in well friction due to polymer viscosity, imposed an additional constraint on the total volume of polymer and water that could be injected into the reservoir altering the total mass of injected fluids.

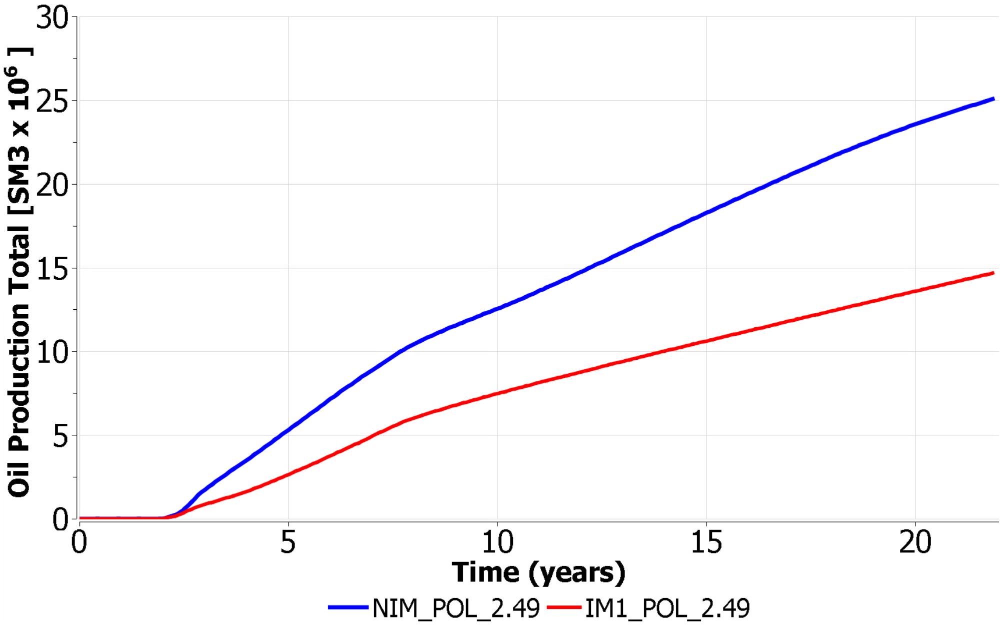

Figure 6.5 – Comparison of final oil production, base case (non-integrated) versus integrated case, considering polymer flooding.

In Figure 6.6 the total amount of water produced is compared for the NIM versus IM1 cases in the polymer injection scenario. Firstly, it is highlighted that the water produced in both cases was significantly lower compared to the water injection scenario. Furthermore, it was observed the same trend, that the IM1 exhibits lower water production than NIM.

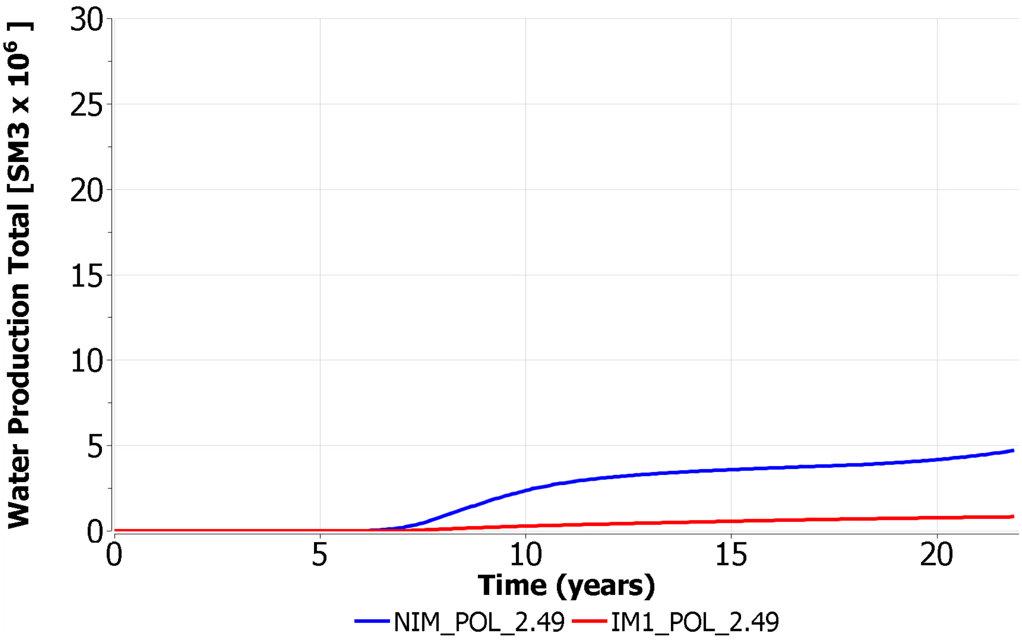

Figure 6.6 – Comparison of total water produced, NIM versus IM1, considering polymer flooding.

6.1.3 Sensitivity Analysis of Polymer Concentration

In this section, it is present the results for sensitivity analysis of polymer concentration for NIM and IM1. It is examined polymer injection concentrations ranging from 0 (representing water flooding) to 0.1, 0.5, 1.0, 2.0, and 2.49 kg/m³ (the previous case).

The results for the total oil recovery, for each concentration, are presented in Figure 6.7. Increasing the polymer concentration did not necessarily lead to an increase in final oil production. The concentration of 0.5 kg/m³ generated the greatest increase in production. The highest polymer concentration significantly affected the total fluid injected and, at 2.0 kg/m³, the results were worse than those obtained with water injection (blue curve).

To confirm the reduction in the mass injected, it is showed the total water injected for each case in Figure 6.8. It is observed that the introduction of even the minimal polymer concentration led to a reduction in the total fluid injected compared to waterflooding.

The decrease in the quantity of fluid injected became more pronounced with higher polymer concentrations. What happened is that, despite reduction in the total fluid injected, the polymer enhanced oil recovery. This enhancement surpassed the loss in the total injected mass up to the concentration of 1.5 kg/m³. Beyond that point, the loss of total injected fluid outweighed the gains from polymer injection. Furthermore, the reduction in fluid injection resulted in a diminished sweep of oil-producing areas. This observed reduction can be attributed to the pressure limits imposed in the injector wells.

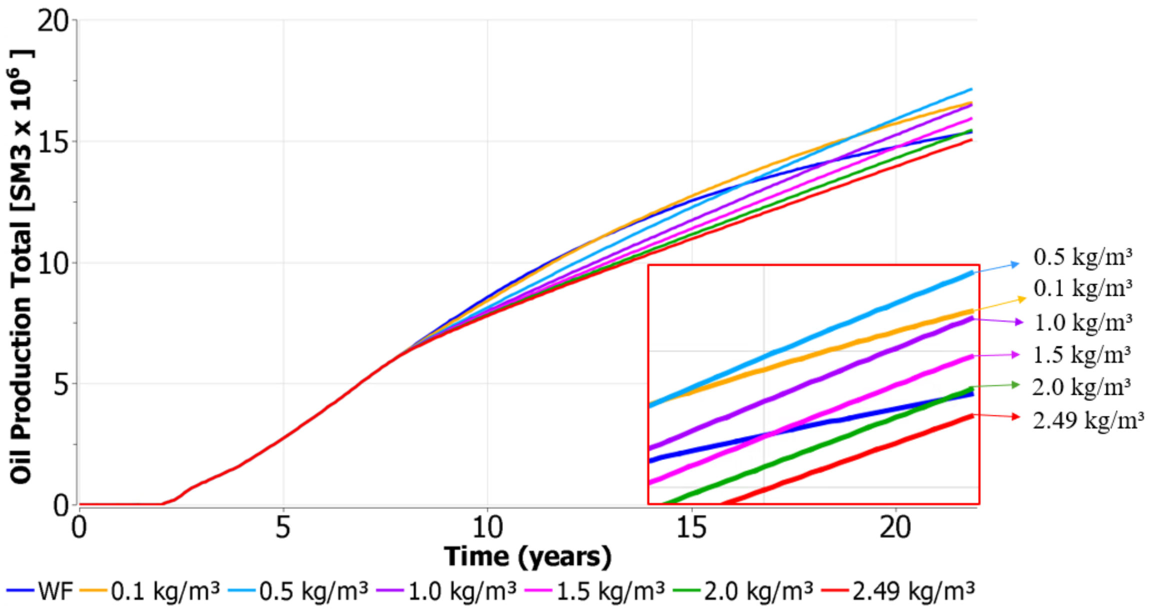

Figure 6.7 – Total oil production for different polymer concentrations considering the Integrated Model (IM1).

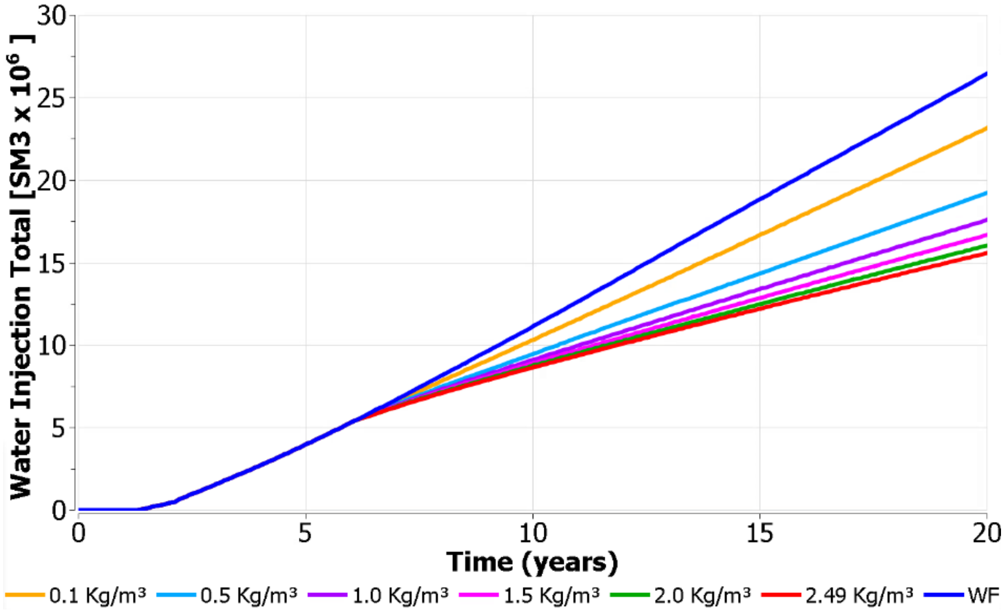

Figure 6.8 – Total water injection for each polymer concentration evaluated (IM1).

Figure 6.9 shows the total amount of produced water for each polymer concentration evaluated in the integrated scenarios. As observed in the plots of total water injected, presented in Figure 6.8, the plots exhibit an inverse relationship between the polymer concentration and the total of fluid produced. This happens due to the lower amount of fluid injected when higher polymer concentrations were used.

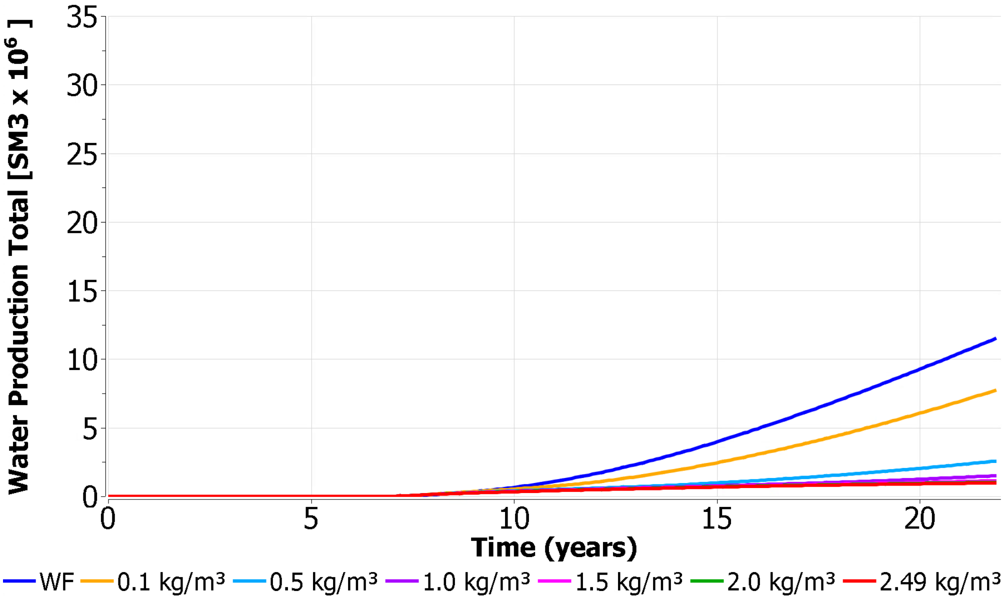

Figure 6.9 – Total water produced for each polymer concentration evaluated (IM1).

Figure 6.10 shows the polymer advance front maps comparing concentrations of 0.5 kg/m³ (left) and 2.49kg/m³ (right) after 20 years of simulation. Despite the lower polymer concentration, the case with 0.5 kg/m³ led to deeper penetration into the reservoir. In the simulation with a concentration of 2.49 kg/m³, a higher concentration of polymer near the injectors can be observed. This might seem counterintuitive, given that a higher concentration of polymer was being injected, which is five times higher in this case. However, as explained earlier, the reduction in the total injected fluid, resulting from the significant pressure drop at the injectors when injecting a viscous polymer fluid, led to less sweeping within the reservoir.

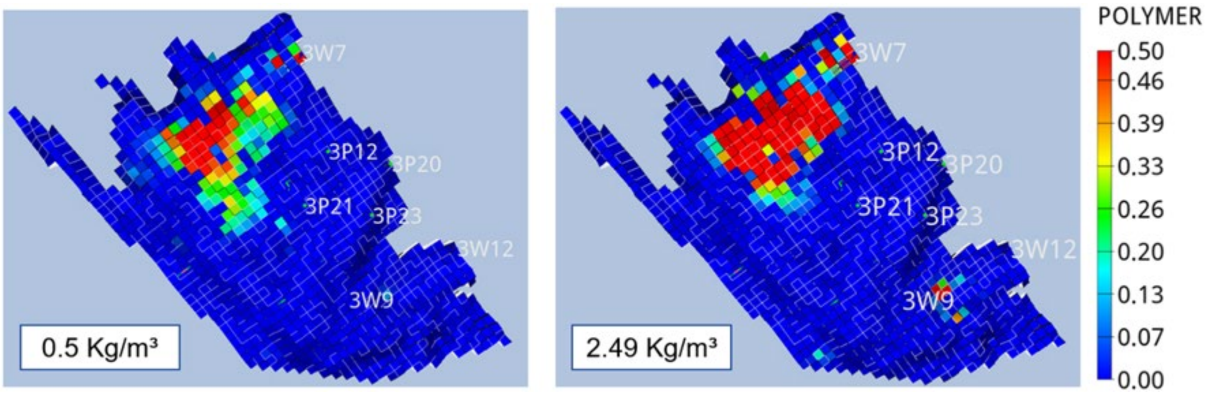

Figure 6.10 – Polymer advance front comparing concentrations 0.5 kg/m³ and 2.49 kg/m³ in the layer k=12.

Figure 6.11 displays the difference in oil production between integrated and non-integrated scenarios as a function of polymer concentration, varying from 0.0 (waterflooding) up to 2.49 kg/m³.

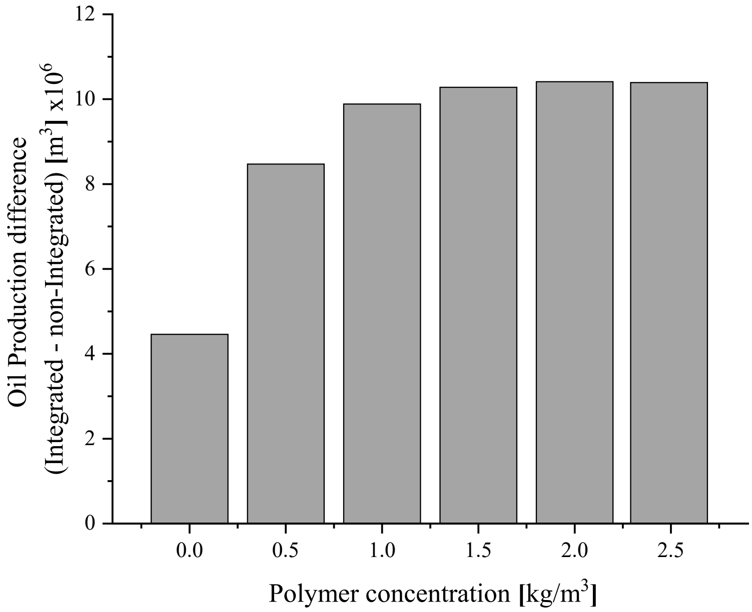

Figure 6.11 – Oil production differences between IM1 and NIM simulations as a function of polymer concentration.

Notably, the difference between integrated and non-integrated in oil production was more pronounced with the increase of polymer concentration until 1.5 kg/m³. Beyond this concentration, the difference in oil production remained steady.

Figure 6.12 presents a comparative analysis of final oil production and its normalization across different polymer concentrations for integrated and non-integrated scenarios, as derived from the simulations in Figure 6.6 and Figure 6.7.

Figure 6.12-a includes the final oil production quantities. An optimal polymer concentration is discernible for both scenarios, with a maximum performance at specific concentrations. Notably, as observed in Figure 6.12-b, the normalized oil production (where each scenario's oil production is divided by its respective maximum) reveals distinct optimal concentrations.

The NIM scenario achieved its maximum recovery at a polymer concentration of approximately 1.2 kg/m³. In contrast, the IM1 obtained a higher oil recovery at a lower concentration of 0.5 kg/m³, which underscores the importance of considering the integration of reservoir and production system interactions. Ignoring such integration may lead to suboptimal operational decisions within the context of these simulations.

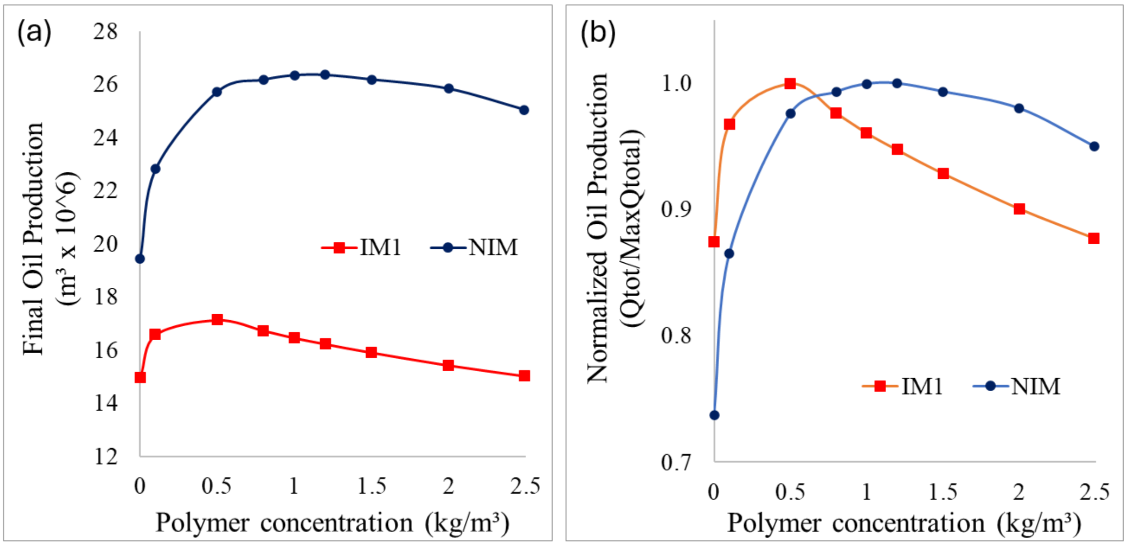

Figure 6.12 – Final oil production (a) and normalized oil production (b) for IM1 and NIM scenarios.

6.1.4 Analysis of Polymer Arrival in Producing Wells

Figure 6.13 shows the WCUT as a function of polymer concentration and breakthrough time (considering detectable concentrations from 0.05 kg/m³). Note that the case with a concentration of 0.5 kg/m³ had a WCUT slightly below 0.2 and the breakthrough time was more than 10 years, that it was, more than 10 years producing without polymer concentration.

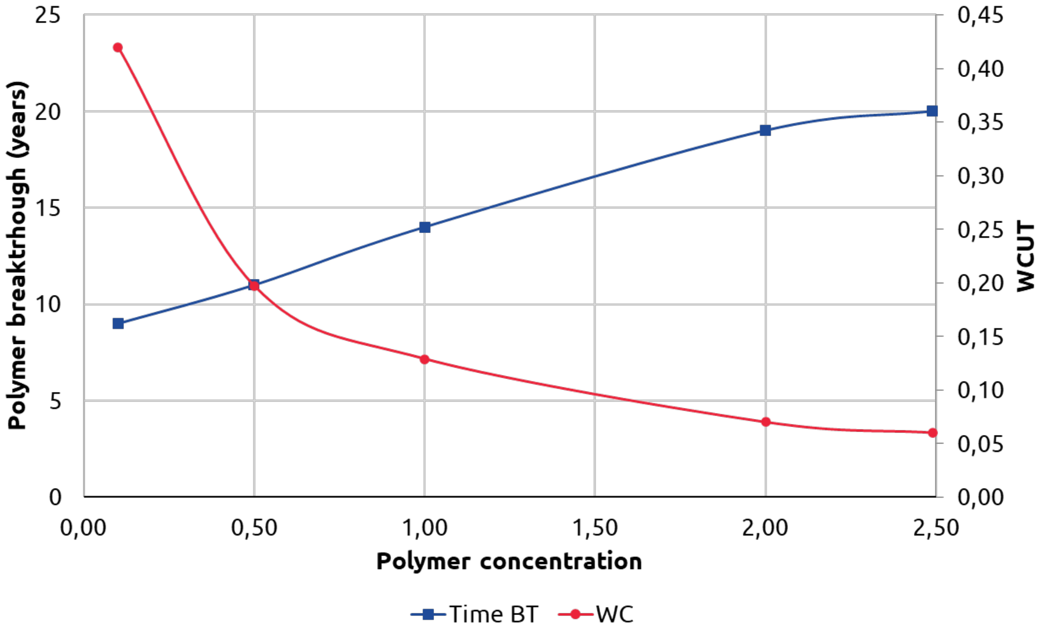

Figure 6.13 – Analysis of polymer concentration arriving at producer wells.

6.2 Effect of the ESP Number of Stages on the Oil Recovery (IM2)

From the previous analyses, it becomes evident that determining the optimal condition for polymer injection was significantly impacted by the established production system configuration. Furthermore, the production systems did not achieve comparable production levels to the NIM, indicating that the PS is undersized.

One possible explanation for this discrepancy is that, although the literature provides initial data for constructing the PS for a reservoir with characteristics similar to the target field in this study, specific factors such as reservoir size, petrophysical characteristics, number of wells, and well positioning can significantly impact the production performance. Therefore, in this section, the number of stages of the ESP was evaluated in terms of oil recovery and economic return.

For clarity and convenience, it will be used the nomenclature ST20, ST37, ST50, and ST80 to represent the pump with 20, 37, 50, and 80 stages, respectively.

The plots presented in Figure 6.14 illustrate the cumulative oil production over a 20-year period, comparing the effects of polymer injection concentration and the number of stages in the pumps. The data is organized across four graphs (a, b, c, and d), each representing a different pump stage scenario ST20, ST37, ST50, and ST80, respectively.

It was verified that, for ST20, the total oil production after 20 years for all cases fell within a lower range compared to the other scenarios. The simulations led to the highest final oil production for the ST20 case (roughly 20 million cubic meters), while it reached approximately

25 million cubic meters for the ST37, ST50, and ST80 cases. Another interesting observation is that the order of the curves (by concentration) was not the same for all stage scenarios, which indicates that the efficiency of polymer injection appears to be influenced by the number of pump stages.

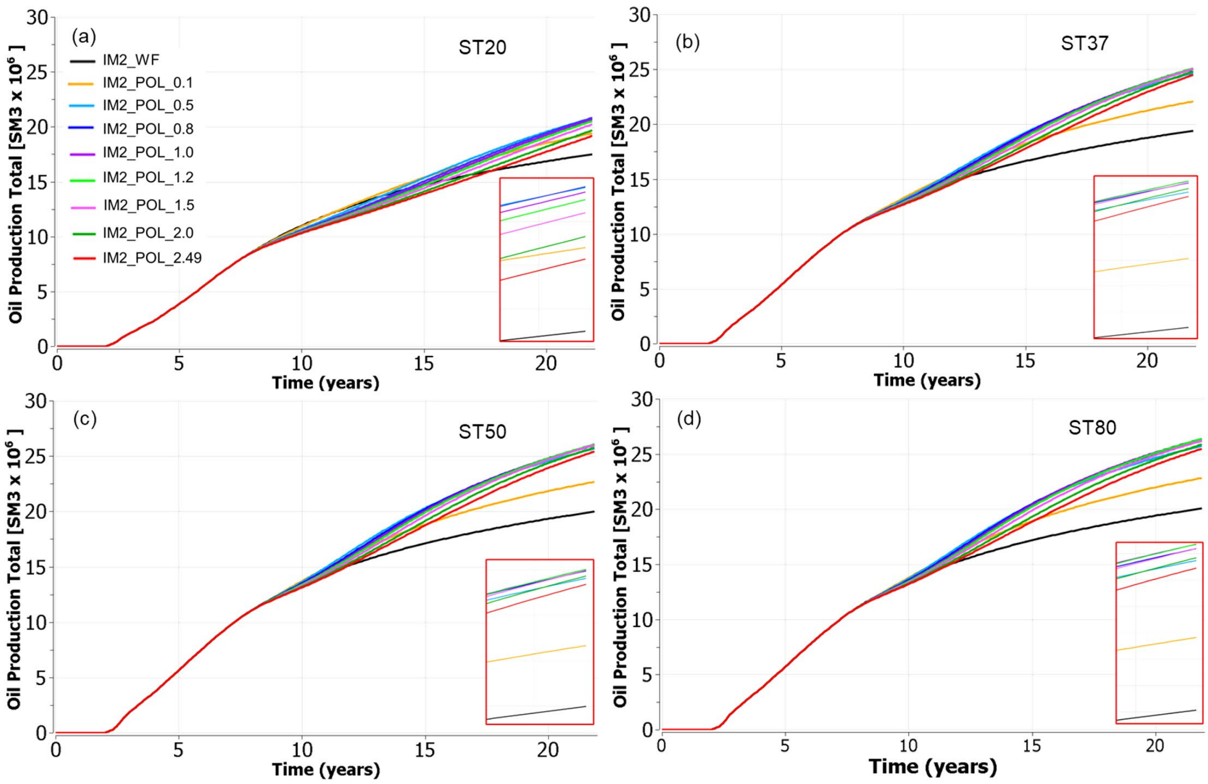

Figure 6.14 – Final oil production for IM2 case considering the pump with (a) 20, (b) 37, (c) 50, and (d) 80 stages for different polymer concentrations.

Figure 6.15 presents a detailed map that illustrates the distribution of polymer concentration, in a central layer (k=12), within the reservoir for simulations a) ST20, b) ST37, c) ST50, and d) ST80 at the end of 20 years of simulation. It is possible to see the polymer spread in red window, which are the regions with higher concentration. A key observation from this map is the enhanced dispersion of polymer treatment front throughout the porous media for the employed higher pump stage. This result highlights the role of well configuration on the fluid dynamics in porous media, thereby influencing the strategic approach to enhanced oil recovery (EOR).

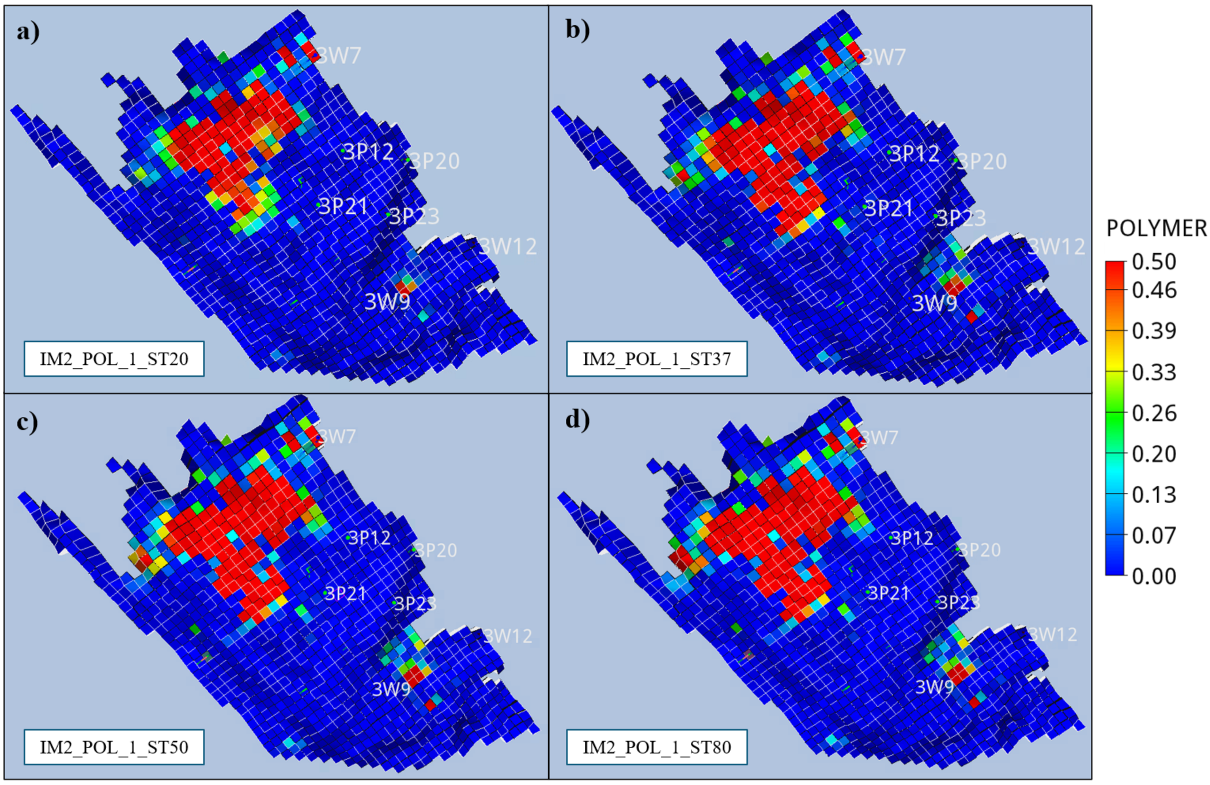

Figure 6.15 – Reservoir polymer concentration distribution for integrated scenarios (IM2) with polymer injection at different pump stage configurations: (a) visualization for the scenario with 20 pump stages; (b) scenario with 37 pump stages; (c) 50 stages, and (d) 80 stages in the layer k=12.

Figure 6.16 shows the final oil production for each scenario, categorized by the number of pump stages, and its relationship with varying polymer concentrations. Across all stage scenarios, there is a noticeable trend where oil recovery ascends with rising polymer concentrations until it reaches a maximum. Beyond this point, the final oil recovery diminishes. Therefore, it becomes clear that each scenario has an optimal point for oil production (a peak at a certain polymer concentration), which shifts with the changing number of stages.

The behavior from the data strongly suggests that identifying the optimal polymer concentration impacts oil recovery efficiency, and this is evidently influenced by the mechanical dynamics of the pumping systems utilized in the production wells.

Another noteworthy observation is that ST37 demonstrated oil production levels on par with the NIM. Furthermore, both the ST50 and ST80 exceeded the production of the NIM, suggesting that the system is now appropriately adjusted. While ST50 and ST80 achieved higher production levels, it is crucial to assess, for practical applications, the potential increase in workload on the pump motor and the potential challenges of operating near its operational limits.

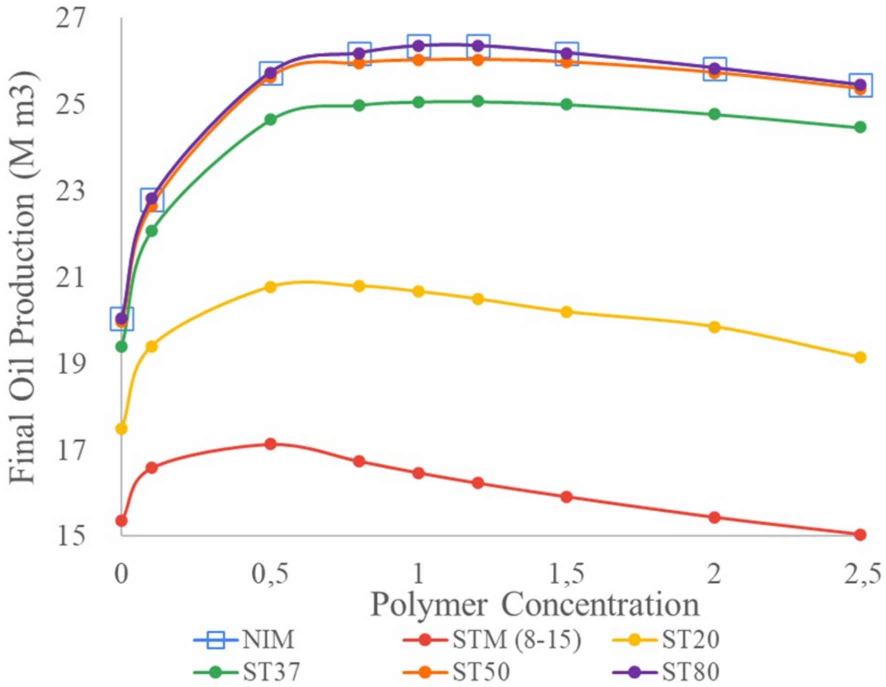

Figure 6.16 – Final oil production for different pump stages.

6.3 Economic Evaluation

In this section, was discussed the economic assessment of operational strategies to determine which yields the best financial return on oil recovery, considering platform, operational, and chemical costs, as described in methodology section.

Figure 6.17 presents the NPV plots for scenarios STM, ST20, and ST37. For all plots, it is observed that, in the initial phase of the project - the first three years, the NPV exhibited a decline. This negative trend is primarily attributable to the upfront capital expenditures and operational costs incurred during the project's development and initial ramp-up phase. The negative cash flows generated during this phase contribute to the diminishing NPV. However, post the initial three-year period, a notable shift occurred as revenues began to exceed costs. This improvement in financial performance was driven by enhanced production levels, therefore elevating the NPV until stabilization.

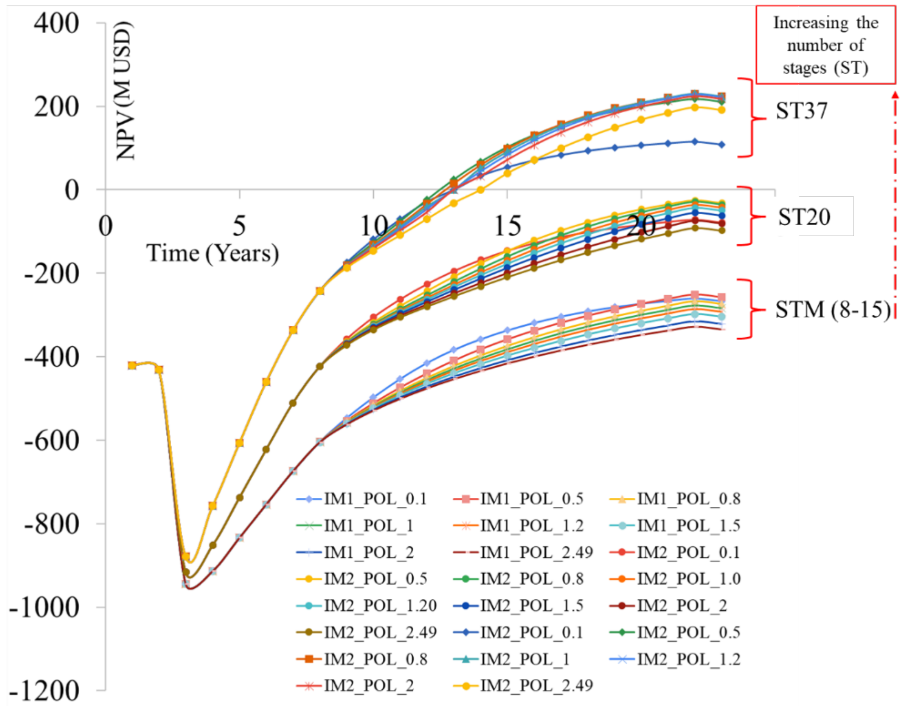

Figure 6.17 – NPV Results for the cases with STM (8-15), ST20, and ST37.

It was observed that a higher number of pump stages correlated with increased production plateaus, and the curves of all three cases are distinctly visible. The simulations for STM and ST20 resulted in negative financial outcomes throughout the simulation period, which indicates that these conditions were not favorable for the well.

Another interesting point it was noted was the divergence in concentrations that yielded the highest financial return for each stage count. There appears to be no uniformity across the different stage scenarios regarding the optimal polymer concentration for maximizing financial returns.

Figure 6.18 shows the NPV plots for the ST50 and ST80 scenarios. The objective is to evaluate the impact of increasing the pump stages number. The results for ST50 and ST80 were on the same level as those for the ST37 simulation. This indicates that simply increasing the number of stages does not necessarily enhance economic return. Another point of concern, which is challenging to quantify, is that operating with a very high number of stages over extended periods demands more power and can overburden the pump's motor, potentially leading to operational issues, unplanned downtimes, and consequent production halts.

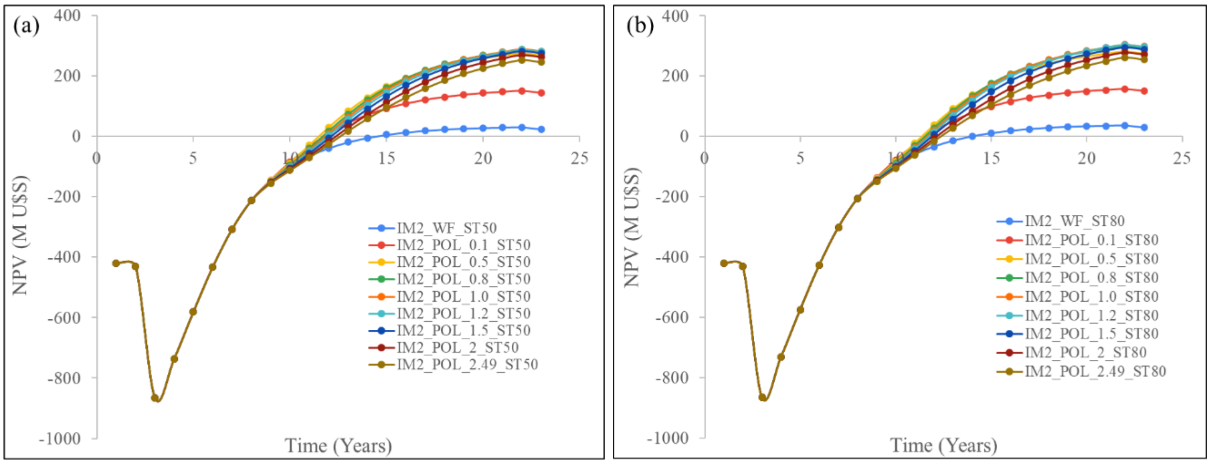

Figure 6.18 – NPV analyses for different number of stages (50 and 80).

In all simulations with varying stage numbers, a consistent observation is that the polymer concentration yielding the maximum financial return shifted with the stage configuration. Figure 6.19 displays the final NPV value for each stage configuration as a function of polymer concentration. This exhibits a trend akin to the oil recovery plots shown in Figure 6.16, but in the context of financial returns.

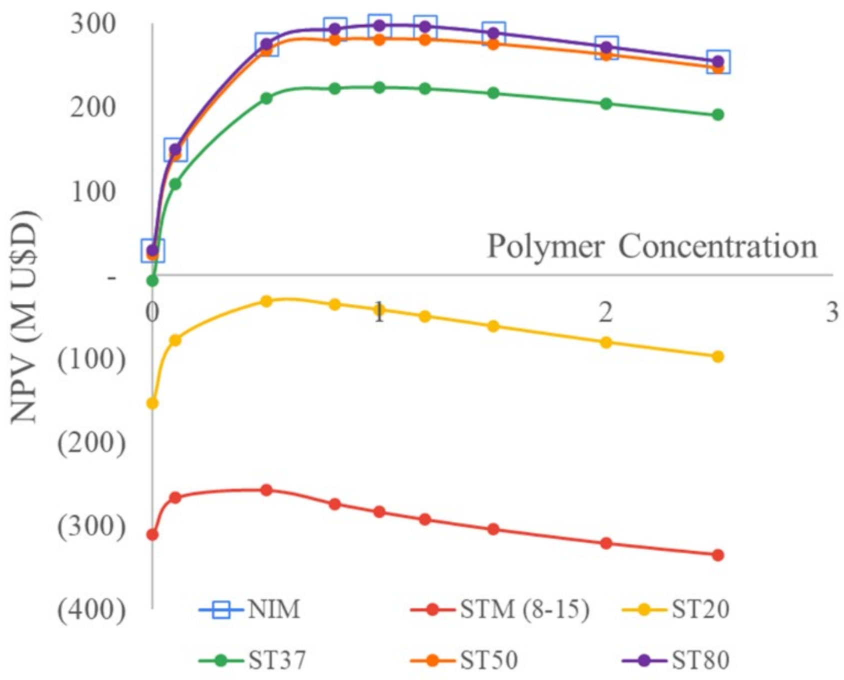

Figure 6.19 – Maximum NPV (20-years) as a function of polymer concentration for each stage configuration.

It is noticeable that, initially, an increase in polymer concentration led to an enhancement in financial returns. Upon reaching a maximum, however, the financial return started to decline, suggesting the existence of an optimal polymer concentration from a financial standpoint.

Importantly, this optimal concentration for maximizing financial returns varied noticeably with the pump configuration.

An intriguing aspect is the observation that the optimal polymer concentration for maximizing oil recovery differed from the concentration for achieving the best financial return. This difference arose when considering the cost implications of the polymer. Although higher polymer concentrations may result in increased oil production, the associated costs may outweigh the economic benefits.

This discrepancy highlights the importance of meticulously balancing mechanical and chemical factors when devising strategies for oil recovery to ensure both operational effectiveness and economic efficiency.

Figure 6.20 shows the final oil production as a function of the number of pump stages for the NIM and IM2 scenarios. Note that the IM2 case converged with the NIM after a certain stage number. This means that, from this moment on, changing the stage number would no longer increase production. Therefore, another parameter of the production system would be chosen for adjustment.

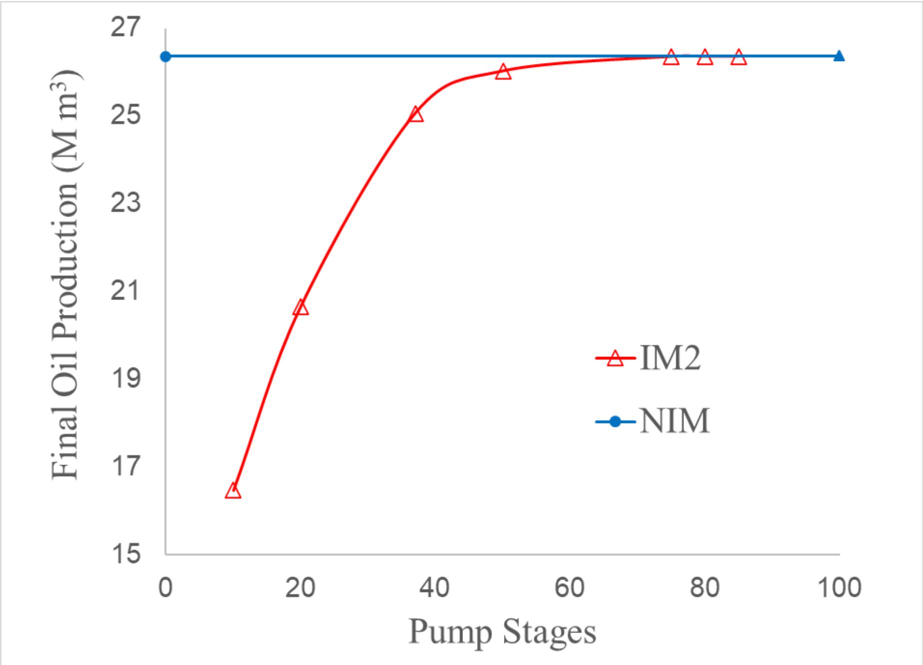

Figure 6.20 – Final oil production as a function of the number of pump stages.

6.4 Summary of Importance of Integration and Economic Evaluation

Up to this point, it was been evaluated the impact of integrating versus not integrating the production system with reservoir simulations, examining both oil production and financial perspectives. It is important to understand that it cannot directly compare the results of integrated and non-integrated scenarios, as they consider different aspects. For instance, the analysis involving variations in the number of pump stages does not correspond to non-integrated scenarios because these do not take well dynamics into account.

When considering the impact of pump stages, it is evident that they play a significant role in determining the polymer concentration that optimizes both oil recovery and financial return. Figure 6.21 illustrates the plots of the optimal polymer concentration for varying pump stages, considering both maximum oil production and the highest final NPV value. Notably, these plots do not align, highlighting a discrepancy that stems from issues such as loss of injectivity with increasing polymer concentration, rising costs, and non-proportional responses in oil recovery.

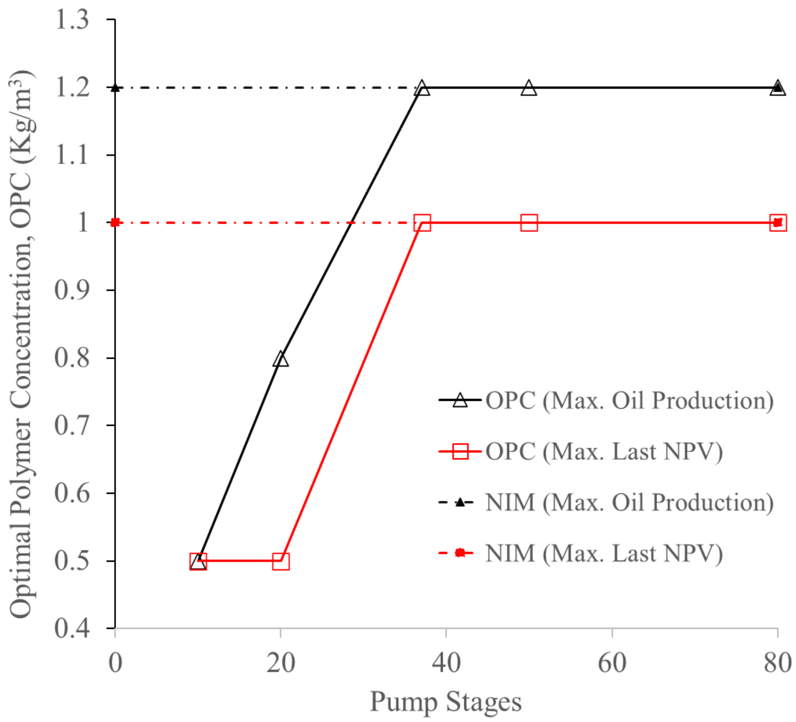

Figure 6.21 – Comparison of optimal polymer concentration (OPC) as a function of the number of stages through maximum oil production and maximum last NPV (from tested values of 0.5, 0,8, 1.0 and 1.2 Kg/m³).

The key insight from the results in Figure 6.21 relates to the approach used in making operational decisions, such as determining the polymer concentration that maximizes Enhanced Oil Recovery (EOR). If well performance is not considered, the chosen polymer concentration might not be truly optimal. More crucially, if the proper pump setup is not considered, simulations can lead to inaccurate optimal operational parameters. This underscores the need to consider both the mechanical setup, the chemical aspects of the operation and the flow in porous media to ensure effective and efficient oil recovery.

6.5 Alternative Approach for Integration

The simulations with the IM1 take an average of 50 minutes, whereas NIMr approach require 15 minutes, representing a 70% reduction in computational time. Figure 6.22 presents the results for the case of water injection and polymer injection. In both scenarios, the curves show total oil production as a function of time, for the NIM, IM1, and NIMr approaches. It is possible to observe that the NIMr curve was very close to the integrated case.

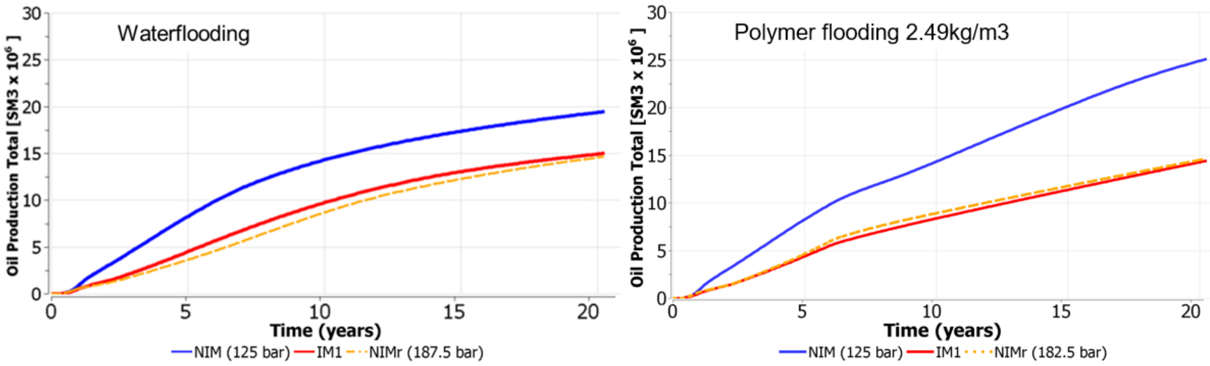

Figure 6.22 – Comparison between integrated and revised BHP scenarios considering waterflooding and polymer flooding.

Figure 6.23 presents a comparison of the final oil production between the IM1 and the NIMr approach across different polymer concentrations. The variation ranged between 0.2 and 2.46%, with the highest difference observed in the scenario of waterflooding. The results indicate that the NIMr approach effectively captures the behavior of total oil production observed in the IM1. This suggests that the NIMr alternative method adequately represents the overall production from the field. In future works, it will be necessary evaluate whether this methodology is effective for water injection and production. An example of how the revised BHP was determined is given in Appendix C.

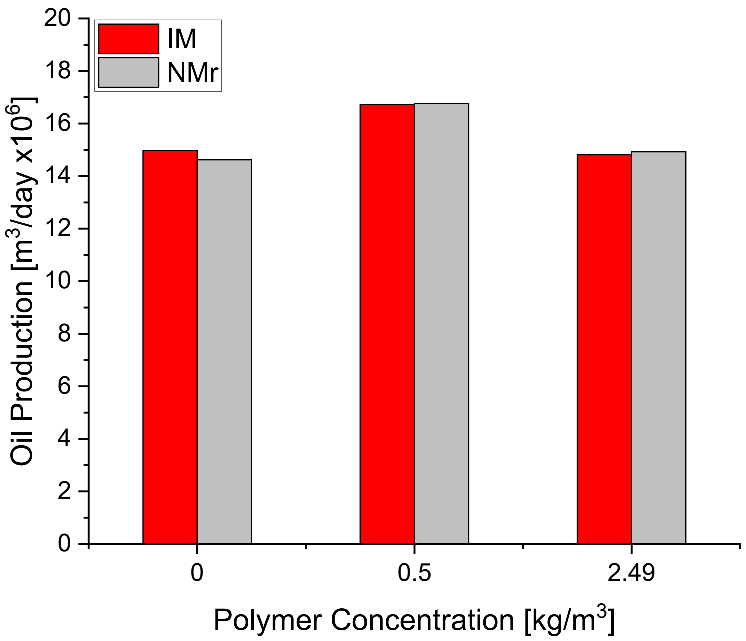

Figure 6.23 – Comparison of final oil production between IM1 and NIMr.

7 CONCLUSIONS

The present study highlights the importance of integration between reservoir and production system in the scenarios of polymer injection in heavy oil reservoirs. The conclusions drawn from the results of this research are given below:

- Integrating the production system with reservoir simulation can lead to a significant difference in oil production, which highlights the importance of adequately considering pressure losses within the production system.
- Comparing water versus polymer injection in the integrated scenarios, it is observed that the polymer injection scenarios were more severely impacted in terms of oil recovery due to the increased pressure loss in injectors and this consequently altered the quantity of fluid injected and the pressure distribution in porous media.

Regarding the case studied in this work:

- Through the sensitivity analyses, optimal polymer concentration for maximizing oil recovery and financial return varied greatly for integrated and non-integrated scenarios. For the non-integrated approach (NIM), polymer concentrations of 0.8 and 1.0 kg/m^3 were the most effective in terms of maximum oil recovery and financial analysis, respectively. However, in the integrated approach (IM1 and IM2), the optimal polymer concentration varied (0.5 to 1.2 kg/m^3), depending on the configuration of the pump stages.
- The characteristics of the production system (in this study case, the number of pump stages) can influence the distribution of polymers in porous media, which consequently affects the optimal polymer concentration for achieving maximum oil recovery and financial return. It was observed that, the higher the number of pump stages, the higher the optimal polymer concentration, reaching a limit of 1.2 kg/m^3.
- The study also compared the integrated model 1 (IM1) with a revised non-integrated approach (NIMr – where BHP was calibrated to minimize the difference to integrated approaches). The results showed that the NIMr approach effectively captured the behavior of total oil production observed in the integrated model, suggesting that it adequately represents the overall production from the field. This was possible due to the behavior of the case studied, with low variation of the conditions (BHP in particular) during the entire simulation time.

The results show that well configuration significantly impacts fluid dynamics in porous media. Furthermore, financial analysis plays a crucial role in balancing the cost implications of different strategies. Our study therefore suggests that simulations with polymer that do not consider integration and economic evaluation can lead to suboptimal operational decisions.

7.1 Recommendations

Based on the experiences acquired during the development of this work, to enhance future research efforts in this field, the following recommendations are proposed:

- Consider the impact of emulsion formation in producer wells on production efficiency and fluid behavior.
- Consider the effects of polymers in reservoirs, including their adsorption behavior, susceptibility to degradation due to shear stress, and their influence on altering residual oil saturation.
- Incorporate a comprehensive study of uncertainties associated with integrated reservoir-production system models.
- Explore other economic scenarios while considering uncertainties inherent in reservoir-production system integration.
- Alternative approaches, such as NIMr methodology, should be explored for estimate the integration effect in non-integrated models.

REFERENCES

Abidin, A. Z., Puspasari, T. Nugroho, W.A. **Polymers for Enhanced Oil Recovery Technology.** Procedia Chem 4, 11–16. 2012. https://doi.org/https://doi.org/10.1016/j.proche.2012.06.002

Al Gahtani, A. **A new Productivity Index Formula for ESP-lifted Wells**, in: SPE Middle East Oil and Gas Show and Conference, MEOS, Proceedings. 2011. https://doi.org/10.2118/141984-ms

Al-Safran, E. M., Brill, J. P. **Applied Multiphase Flow in Pipes and Flow Assurance: Oil and Gas Production.** Society of Petroleum Engineers. 2017. https://doi.org/10.2118/9781613994924

Andreolli, I. **Introdução à Elevação e Escoamento Monofásico e Multifásico de Petróleo.** Rio de Janeiro. Interciência. 2016.

Andrews, K. **How Does an Electric Submersible Pump (ESP) Work** 2024. https://kimray.com/training/how-does-electric-submersible-pump-esp-work. Accessed on April 18, 2024.

Beall, R., Sheth, K., Olsen, H. **An Integrated Solution Enabling Allocation of Heavy Oil in the Peregrino Field.** 2011. https://doi.org/10.4043/21790-ms

Beggs, H. D., Brill, J. R. **Study of Two-Phase Flow in Inclined Pipes.** JPT, Journal of Petroleum Technology 25, 607–617. 1973. https://doi.org/10.2118/4007-PA

Botechia, V. E., Barreto, C. E. A. G., Lamas, L.F., Schiozer, D. J. **Evaluation of Alternate Water-Polymer Injection Parameters Using Numerical Simulation.** Brazilian Journal of Petroleum and Gas 13, 093–102. 2019. http://dx.doi.org/10.5419/bjpg2019-0009

Cao, H., Samier, P., Kalunga, H. M., Detige, E., Obi, E. **A Fully Coupled Network Model, Practical Issues and Comprehensive Comparison with Other Integrated Models on Field Cases**, in: SPE Reservoir Simulation Symposium. Society of Petroleum Engineers. 2015. https://doi.org/10.2118/173251-MS

Castro, V., Pastre, L., Marins, J. **ESP Technology Improvements in Peregrino field**, in: Society of Petroleum Engineers - SPE Gulf Coast Section Electric Submersible Pumps Symposium 2019, ESP 2019. 2019. https://doi.org/10.2118/194401-ms

Chen, S. **Petroleum Production Engineering,** in: Springer Handbooks. 2017. https://doi.org/10.1007/978-3-319-49347-3_14

Ding, D. Y., Wu, Y.S., Jeannin, L. **Efficient Simulation of Hydraulic Fractured Wells in Unconventional Reservoirs.** Journal of Petroleum Science Engineering 122, 631–642. 2014. https://doi.org/10.1016/J.PETROL.2014.09.005

Gao, C. H. **Advances of Polymer Flood in Heavy Oil Recovery**, in: Heavy Oil Conference and Exhibition, Kuwait City, Kuwait. SPE. 2011. https://doi.org/10.2118/150384-MS

Gbadamosi, A., Patil, S., Kamal, M. S., Adewunmi, A. A., Yusuff, A. S., Agi, A., Oseh, J. **Application of Polymers for Chemical Enhanced Oil Recovery: A Review.** Polymers (Basel). 2022. https://doi.org/10.3390/polym14071433

Gbadamosi, A. O., Junin, R., Muhammad, ·, Manan, A., Agi, · Augustine, Yusuff, A. S. **An Overview of Chemical Enhanced oil Recovery: Recent Advances and Prospects.** Int. Nano Letters 2019 9:3 9, 171–202. 2019. https://doi.org/10.1007/S40089-019-0272-8

George Yadigaroglu, Geoffrey F. Hewitt, **Introduction to Multiphase Flow, Introduction to Multiphase Flow.** Springer International Publishing, Cham. 2018**.** https://doi.org/10.1007/978-3-319-58718-9

Ghorayeb, K., Holmes, J., Torrens, R., Grewal, B. **A General-Purpose Controller for Coupling Multiple Reservoir Simulations and Surface Facility Networks**, in: SPE Reservoir Simulation Symposium, Houston, Texas. SPE. 2003. https://doi.org/10.2118/79702-MS

Guo, B., Lyons, W.C., Ghalambor, A. **Artificial Lift Methods, in: Petroleum Production Engineering.** 2007 https://doi.org/10.1016/b978-075068270-1/50074-8

Hiebert, A., Khoshkbarchi, M., Sammon, P., Alves, I., Rodrigues, J. R., Belien, A., Howell, B., Saaf, F., Valvatne, P. **An Advanced Framework for Simulating Connected Reservoirs,**

Wells and Production Facilities. SPE Reservoir Simulation Symposium. Texas, EUA: Society of Petroleum Engineers. 2011. https://doi.org/10.2118/141012-MS

Hohendorff Filho, J.C. Von, Schiozer, D.J., **Integrated Optimization of Multiple Reservoirs in Shared Production Systems.** International Journal of Oil, Gas and Coal Technology 30, 109. 2022. https://doi.org/10.1504/IJOGCT.2022.122638

Hohendorff Filho, J.C. Von, Schiozer, D.J., 2022b. **Integrated optimisation of multiple reservoirs in shared production systems.** International Journal of Oil, Gas and Coal Technology 30, 109. https://doi.org/10.1504/IJOGCT.2022.122638

Isaev, A. A., Takhautdinov, R. S., Yunusov, I. M., Novikov, M. G., Malykhin, V. I. **Enhanced Oil Recovery Techniques to Develop Mature Oilfields. Society of Petroleum Engineers -** SPE Annual Caspian Technical Conference 2022, CTC 2022. 2022. https://doi.org/10.2118/212140-MS

Jansen, J. D. **Nodal Analysis of Oil and Gas Production Systems**, Nodal Analysis of Oil and Gas Production Systems. 2017. https://doi.org/10.2118/9781613995648

Jia, H. **Effect of Reservoir Heterogeneity on air Injection Performance in a Light oil Reservoir.** Petroleum 4, 15–24. 2018. https://doi.org/10.1016/J.PETLM.2017.10.006

Joel Romero, O., Hupp, A. **Subsea Electrical Submersible Pump Significance in Petroleum Offshore Production.** Journal Energy Resource Technol 136. 2014. https://doi.org/10.1115/1.4025258

Kharisov, R. Y., Folomeev, A. E., Sharifullin, A. R., Bulgakova, G. T., Telin, A. G. **Integrated Approach to Acid Treatment Optimization in Carbonate Reservoirs.** Energy and Fuels 26, 2621–2630. 2012. https://doi.org/10.1021/ef201388p

Kristoffersen, Ø., Stanko, M., Hoffmann, A. **Short Term Production Optimization Using a Model of the Peregrino Field**, Brazil, in: OTC Brasil 2017. 2017. https://doi.org/10.4043/27995-ms

Lake, L. W. **Petroleum Engineering Handbook.** Society of Petroleum Enginners. 2006.

Lamas, L. F., Botechia, V. E., Correia, M. G., Schiozer, D. J., Delshad, M., **Influence of Polymer Properties on Selection of Production Strategy for a Heavy Oil Field.** Journal Petroleum Science Engineering 163, 110–118. 2018. https://doi.org/10.1016/j.petrol.2017.12.074

Lamas, L. F., Botechia, V. E., Schiozer, D. J., Rocha, M. L., Delshad, M. **Application of Polymer Flooding in the Revitalization of a Mature Heavy Oil Field.** Journal Petroleum Science Engineering 204, 108695. 2021. https://doi.org/10.1016/J.PETROL.2021.108695

Lea, J. F., Rowlan, L. **Nodal Analysis: Analyzing loaded wells, in: Lea, J.F., Rowlan, L. (Eds.), Gas Well Deliquification.** Gulf Professional Publishing, pp. 37–45. 2019. https://doi.org/10.1016/B978-0-12-815897-5.00004-4

Li, Z., Delshad, M., Lotfollahi, M., Koh, H., Luo, H., Chang, H.L., Zhang, J., Dempsey, P., Lucas-Clements, C., Brennan, B. **Polymer Flooding of a Heavy Oil Reservoir with an Active Aquifer**, in: Proceedings - SPE Symposium on Improved Oil Recovery. 2014 https://doi.org/10.2118/169149-ms

Lopes, F. R. **Estudo Experimental de Dano de Formação em Meios Porosos (Experimental Study of Formation Damage on Porous Media)** (Master Tesis). 2012. Universidade Estadual de Campinas (UNICAMP), Campinas.

Manshad, A. K., Jabbari, M., Mohammadi, A. H. **Oil Production Optimization via Optimum Artificial Lift Design**, in: Heavy Oil: Characteristics, Production and Emerging Technologies. 2017.

Nguyen, T., & Nguyen, T. (2020). Artificial lift selection methodology for vertical and horizontal wells in conventional and unconventional reservoirs. Artificial Lift Methods: Design, Practices, and Applications, 317-347.

Noonan, S. **Technology Focus: Artificial Lift.** Journal of Petroleum Technology 64. 2012. https://doi.org/10.2118/0712-0084-jpt

Olsen, H., Sheth, K., Pessoa, R., Rutter, R., Crossley, A. **Successful Production Allocation Through ESP Performance in Peregrino field**, in: SPE Latin American and Caribbean Petroleum Engineering Conference Proceedings. 2012.https://doi.org/10.2118/152391-ms

Olsen, H., Sheth, K., Pessoa, R.F., Okita, R., Crossley, A., Martinez, I. **ESP Assisted Production Allocation in Peregrino Field**, in: Proceedings of the Annual Offshore Technology Conference. 2011. https://doi.org/10.4043/22579-ms

Pastre, L., Biazussi, J., Verde, W. M., Marins, J., Melchuna, A., Cowie, M., Vergara, L., Navarro, I., Lemos, D., Alfonzo, A., Ramos, L., Bannwart, A. **Understanding ESP Performance Under High Viscous Applications and Emulsion Production**, in: Proceedings of the Annual Offshore Technology Conference. 2022. https://doi.org/10.4043/31839-MS

Qin, L., Arjomand, E., Myers, M. B., Otto, C., Pejcic, B., Heath, C., Saeedi, A., Wood, C. **Mechanistic Aspects of Polymeric Relative Permeability Modifier Adsorption onto Carbonate Rocks.** Energy and Fuels 34, 12065–12077. 2020. https://doi.org/10.1021/acs.energyfuels.0c01590

Rellegadla, S., Prajapat, G., Agrawal, A. **Polymers for enhanced oil recovery: fundamentals and selection criteria.** Appl Microbiol Biotechnol 101, 4387–4402. 2017. https://doi.org/10.1007/s00253-017-8307-4

Rosa, A. J., de Souza Carvalho, R., Xavier, J. A. D. **Engenharia de reservatórios de petróleo.** Interciência. 2006.

Rotondi, M., Cominelli, A., Di Giorgio, C., Rossi, R., Vignati, E., Carati, B., 2008. **The Benefits of Integrated Asset Modeling: Lesson Learned from Field Cases**, in: Europec/EAGE Conference and Exhibition, Rome, Italy. SPE. 2008. https://doi.org/10.2118/113831-MS

Schlumberger. **REDA Electric Submersible Pump Technology** - ESP Catalog. 2005.

Silveira, B. M. O. et al. **Model-Based Analysis to Evaluate the Effect of Polymer Properties and Physical Phenomena on Polymer Flooding Operations**. Brazilian Journal of Petroleum and Gas, v. 18, n. 1, 2024. http://dx.doi.org/10.5419/bjpg2024-0003

Su, S. J., Patacchini, L., Mohmed, F., Farouk, M., Ouzzane, D., Draoui, E., Torrens, R., Amoudruz, P. **Coupling Production and Injection Systems with Multiple Reservoir Models: A Novel Method of Optimizing Development Strategies in a Mature Giant Oilfield**, in: Society of Petroleum Engineers - Abu Dhabi International Petroleum Exhibition and Conference 2016. 2016. https://doi.org/10.2118/183153-ms

Thomas, A. **Essentials of Polymer Flooding**, in: Essentials of Polymer Flooding Technique. 2019. https://doi.org/10.1002/9781119537632.oth1

Victorino, I. R. de S., von Hohendorff Filho, J. C., de Castro, M. S., de Mello, S. F., Schiozer, D.J. **Influence of Well and Gathering Systems Parameters on Integrated Petroleum Reservoir and Production System Simulations.** Journal of the Brazilian Society of Mechanical Sciences and Engineering 40, 435. 2018.

Victorino, I. R. S., João, N.A., Filho, o C.V.H., Castro, M.S., Schiozer, D.J., 2021. **Definition of an Oilfield Production Strategy Through Integrated Simulation of Manifolded Production System and Reservoir.** International Journal of Oil, Gas and Coal Technology 28, 387. 2021. https://doi.org/10.1504/IJOGCT.2021.118843

Victorino, I. R. S., Hohendorff Filho, J. C. V., Castro, M. S., Schiozer, D. J. **Impact of Integration of the Production Systems and Reservoir of a Benchmark Based on Carbonate Fields.** Journal Energy Resource Technology 144. 2022. https://doi.org/10.1115/1.4053435

Yadigaroglu, G., Hewitt, G. F. **Introduction to Multiphase Flow, Introduction to Multiphase Flow.** Springer International Publishing, Cham. 2018**.** https://doi.org/10.1007/978-3-319-58718-9

Zhao, Y., Yin, S., Seright, R. S., Ning, S., Zhang, Y., Bai, B. **Enhancing Heavy-oil-recovery Efficiency by Combining Low-Salinity-Water and Polymer Flooding.** SPE Journal 26. 2021 https://doi.org/10.2118/204220-PA

Zhou, W., Banerjee, R., Proano, E. **Nodal Analysis for Unconventional Reservoirs—Principles and Application.** SPE Journal 21, 245–255. 2016. https://doi.org/10.2118/171768-PA

APPENDIX A – EXPLANATIONS ABOUT ELECTRICAL SUBMERSIBLE PUMPS (ESPs)

This section will provide an overview of Electrical Submersible Pumps (ESPs) and their application in the oil industry.

About the ESP use in Oilfield

Electrical submersible pumps are widely used in the oil field industry, due his versatility and high operational range. His primary role is to enhance fluid elevation. This is achieved by transferring kinetic energy to the fluid using centrifugal force, and subsequently transforming it into potential energy in terms of pressure.

The ESP system consists of several components, including the pump, motor, seal section, and power cable. The motor provides the necessary power to drive the pump and is usually located above the pump in a separate housing. The pump is responsible for creating the centrifugal force and moving the fluid. The seal section ensures that the pump and motor are properly sealed to prevent fluid leakage. The power cable connects the motor to the power source, allowing electricity to be supplied to the motor. In an ESP operation, the pump is installed at the bottom of the wellbore and is submerged in the fluid it needs to lift. The pump's impellers rotate rapidly, causing the fluid to be drawn in and propelled upwards. This process allows for efficient and continuous well fluids lifting (Schlumberger, 2005).

Figure A.1 illustrates the effect of ESP installation on the Outflow performance Relationship (OPR). It is possible to observe that in the case with ESP installed the operational point, represented by the intersection between the two plots (OPR and IPR) is dislocated to the right, achieving a higher flow rate (Al Gahtani, 2011).

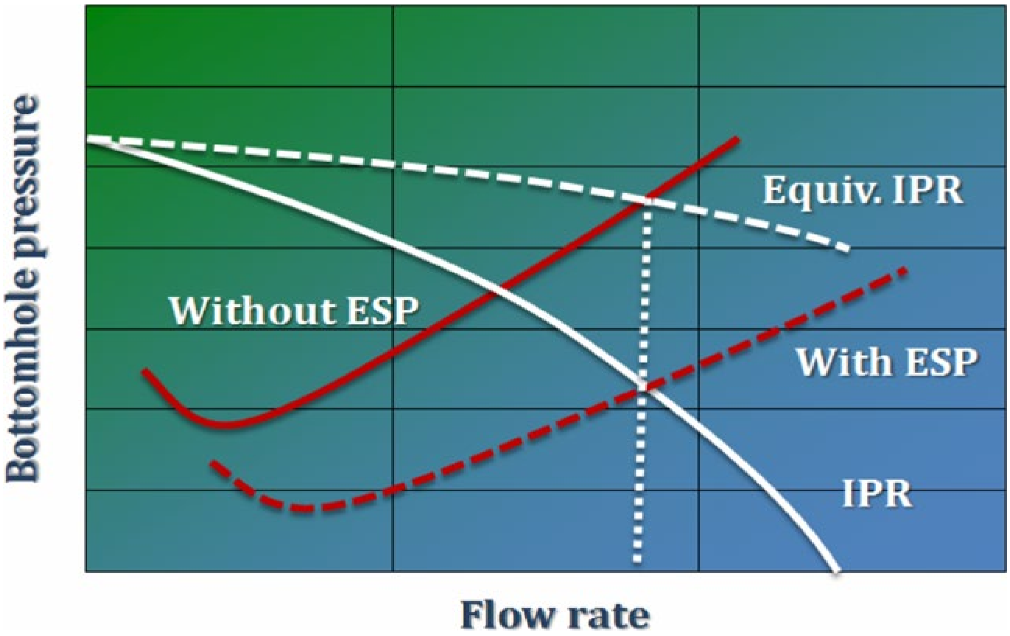

Figure A. 1- Effect of ESP on OPR (Al Gahtani, 2011)

Centrifugal Pump (Impeller and Diffuser) - Stages

The stages of the centrifugal pump are the elements responsible to increase the pressure of the fluid. Each stage is made up of a rotating impeller and stationary diffuser, as illustrated in Figure A.2. The stages can be stacked to incrementally increase the pressure until the desired flow rate is achieved.

The fluid travels through a rotating impeller which increases its kinetic energy, or velocity. It then enters the diffuser, converting the energy to potential energy which raises the discharge pressure. The fluid repeats the process in each stage of the pump, until the fluid reaches the design discharge pressure. The increase in pressure is called the total developed head (TDH) of the pump. The impellers are crucial to the operation of an ESP because they determine the flow rate.

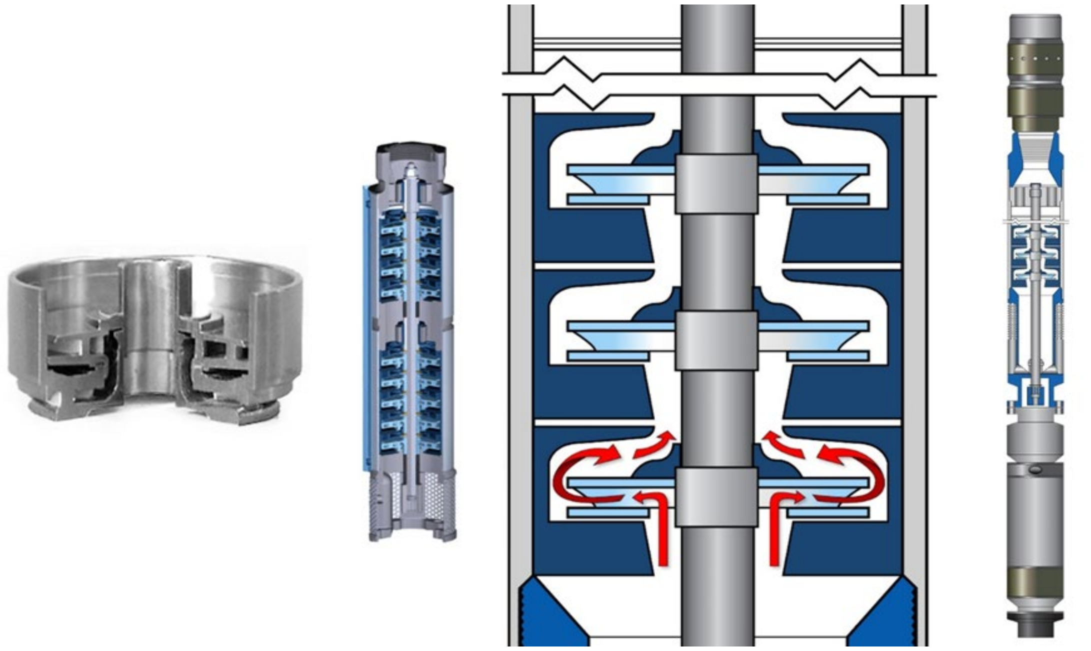

Figure A. 2 - Effect of ESP on OPR (Andrews, 2024).

APPENDIX B – PUMP PERFORMANCE CURVE

This appendix presented the performance and variable speed characteristics curves of the pumps at different stage numbers used in the study. Table B.1 displayed a summary of the modeled cases, listing the respective nomenclatures and corresponding figures.

Table B.1 – Resume of nomenclature for the modeled case and the respective stage number.

Nomenclature	Wells x Stages	Figure
STM	1 x 8	Figure B.1
	1 x 10	Figure B.2
	2 x 12	Figure B.3
ST37	4 x 37	Figure B.4
ST50	4 x 50	Figure B.5
ST80	4 x 80	Figure B.6

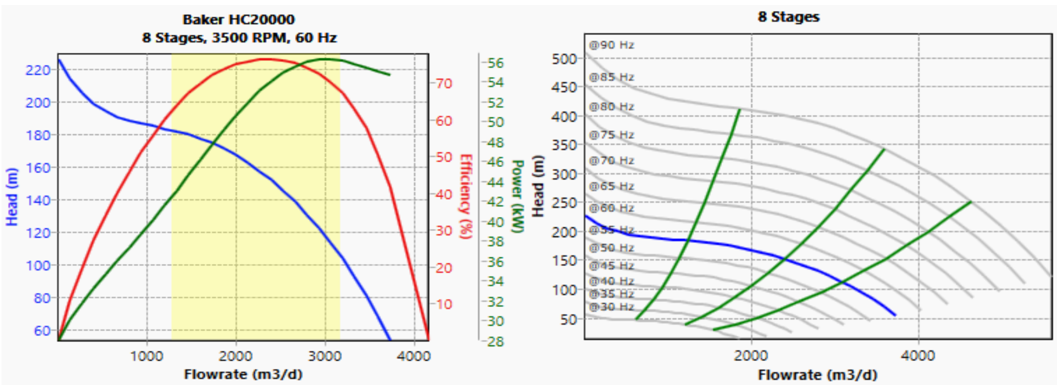

Figure B.1 – Pump performance (left) and variable speed (right) curves for the pump with 8 stages.

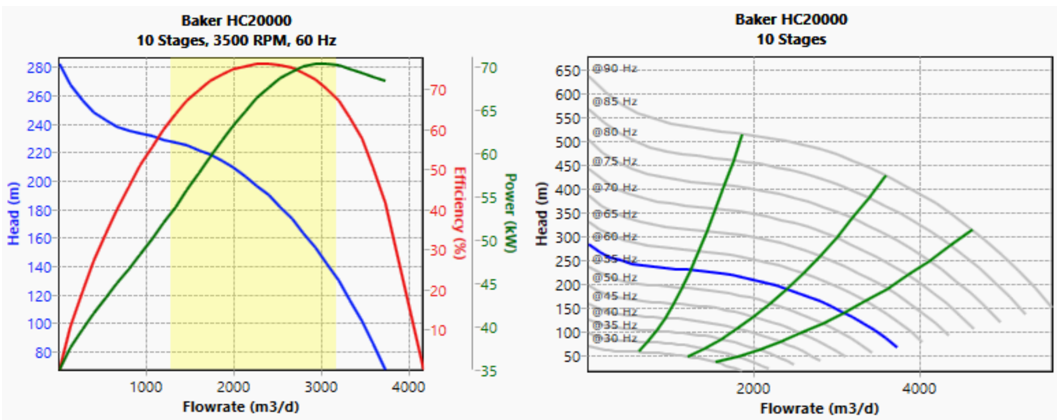

Figure B.2 – Pump performance (left) and variable speed (right) curves for the pump with 10 stages.

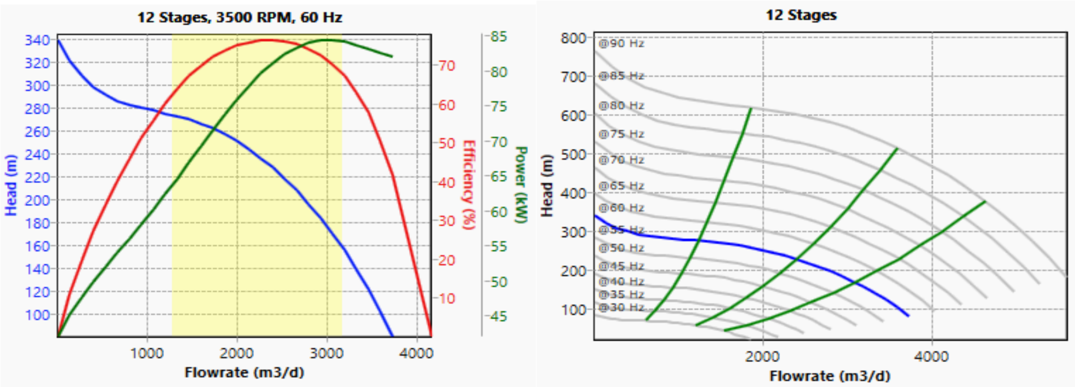

Figure B.3 – Pump performance (left) and variable speed (right) curves for the pump with 12 stages.

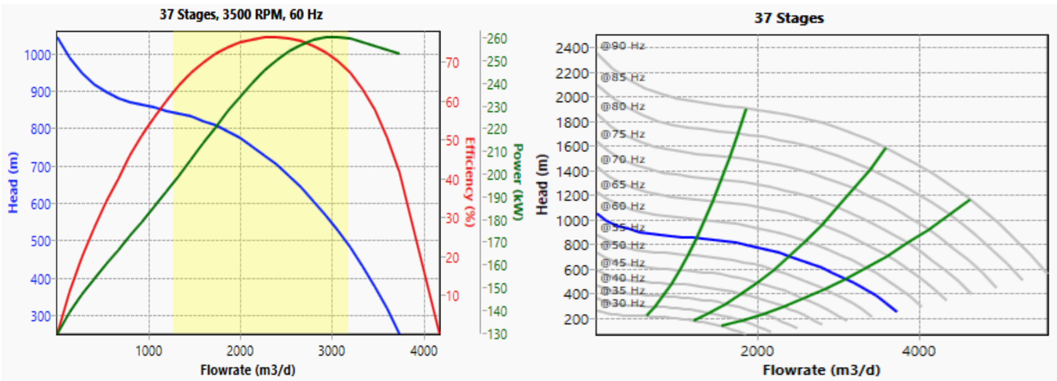

Figure B.4 – Pump performance (left) and variable speed (right) curves for the pump with 37 stages.

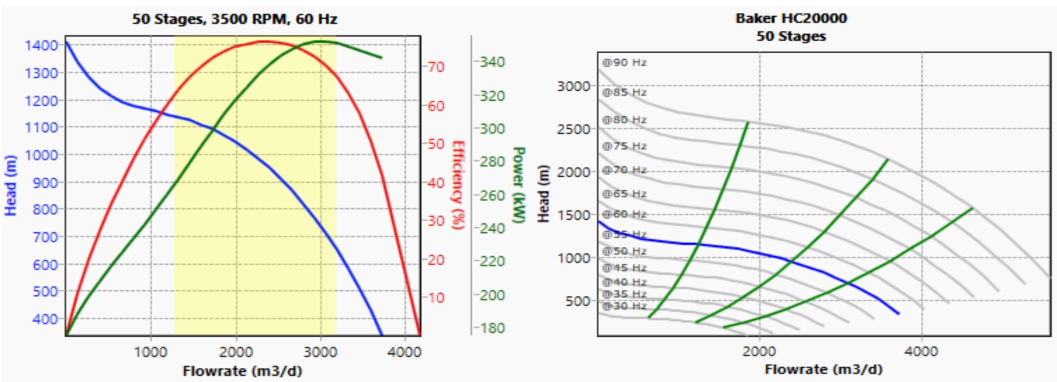

Figure B.5 – Pump performance (left) and variable speed (right) curves for the pump with 50 stages.

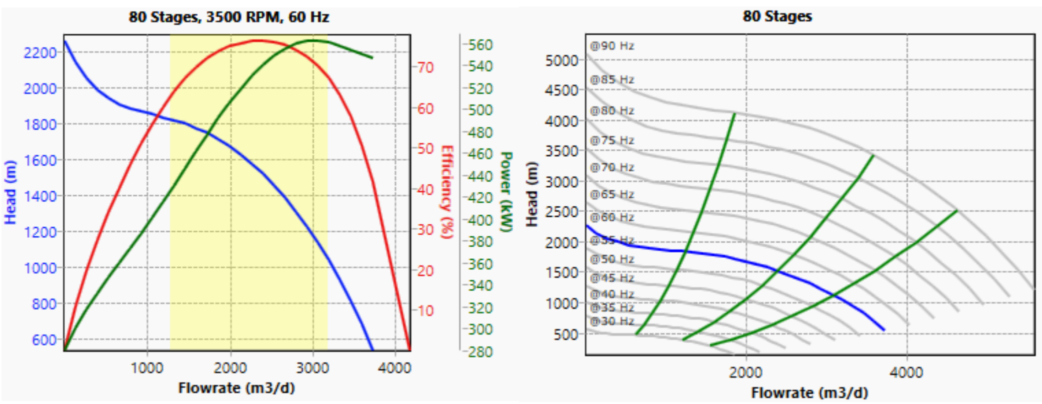

Figure B.6 – Pump performance (left) and variable speed (right) curves for the pump with 80 stages.